Ultrasound in medicine and biology

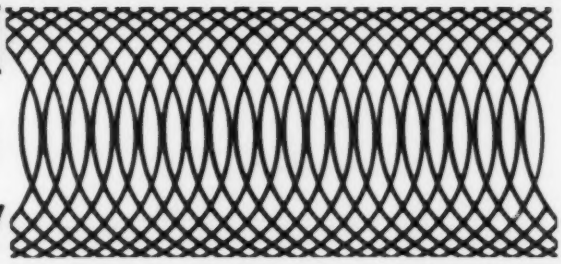

~~Supplement to~~ *Ultrasound in Medicine and Biology*, Volume 20, Number 3, 1994

Author–Subject Index Volume 19 (1993)

Compiled by

Michael Halliwell
Department of Medical Physics, Bristol General Hospital, Bristol BS1 6SY, United Kingdom

PERGAMON

ULTRASOUND IN MEDICINE AND BIOLOGY

WORLD FEDERATION FOR ULTRASOUND IN MEDICINE AND BIOLOGY

President: M. FUKUDA, *Sapporo, Japan*
Vice-President: H. TAKEUCHI, *Tokyo, Japan*
Past-President: F. WEILL, *Besançon, France*
President-Elect: B. GOLDBERG, *Philadelphia, USA*
Treasurer: W. O'BRIEN, *Urbana, USA*
Secretary: D. ROBINSON, *Chatswood, Australia*
Editor-in-Chief of the Journal: P. N. T. WELLS, *Bristol, UK*
Councillors: C. R. B. MERRITT, *New Orleans, USA*
H. WATANABE, *Kyoto, Japan*
H. LUTZ, *Bayreuth, Germany*
G. CERRI, *São Paulo, Brazil*
W. WIBISONO, *Jakarta, Indonesia*
S. HANCKE, *Hellerup, Denmark*
M. ZISKIN, *Philadelphia, USA*
S. EIK-NES, *Trondheim, Norway*

AFFILIATED SOCIETIES

American Institute of Ultrasound in Medicine (AIUM), L. Nelson, Secretary, 14750 Sweitzer Lane, Suite 100, Laurel, MD 20707, USA

Asian Federation of Societies for Ultrasound in Medicine and Biology (AFSUMB), K. Nakayama, Secretary, Faculty of Science and Technology, Sophia University, 7-1 Kioicho, Chiyoda-ku, Tokyo, Japan

Australasian Society for Ultrasound in Medicine (ASUM), F. Adams, Executive Secretary, 2/181 High Street, Willoughby, NSW 2068, Australia

European Federation of Societies for Ultrasound in Medicine and Biology (EFSUMB), L. Surry, Executive Secretary, The Clerestory, 2 Mount Park Road, Ealing, London, W5 2RP, UK

Latin-American Federation of Societies for Ultrasound in Medicine and Biology (FLAUS), G. G. Cerri, Permanent Secretary, Av. Paulista, 491 13° conj. 132, CEP 01311, São Paulo, Brazil

Mediterranean and African Society for Ultrasound (MASU), H. A. Gharbi, President, Hopital d'Enfants, Place Bab Saadoun, 1007 Tunis Jabbari, Tunisia

Societas Internationalis pro Diagnostica Ultrasonica in Ophthalmologia (SIDUO), G. Hasenfratz, Secretary, University Eye Hospital, Wuerzburg, Josef-Schneider-Str. 11, D-8700 Wuerzburg, Germany

South African Medical Ultrasound Society (SAMUS), M. Jacobson, Secretary, Box 93499, Yeoville 2143, Republic of South Africa

---

Production Editor: L. Johnson.

Publishing, Advertising, and Subscription Offices: Elsevier Science Inc., 660 White Plains Road, Tarrytown, NY 10591-5153, USA, E-mail Address: ESUK.USA@ELSEVIER.COM; or Elsevier Science Ltd, The Boulevard, Langford Lane, Kidlington, Oxford, OX5 1GB, United Kingdom.

Published 9 per Annum. *Annual Institutional Subscription Rates* (1994): North, Central and South America, US$575.00, Rest of World £375.00. Sterling prices exclude VAT. Non-VAT registered customers in the European Community will be charged the appropriate VAT in addition to the price listed. Prices include postage and insurance and are subject to change without notice. Members of the World Federation for Ultrasound in Medicine and Biology may order personal subscriptions at a concessional rate; details of these rates are available upon request.

Pergamon

Ultrasound in Med. & Biol., Vol. 20, Suppl., pp. 1–45, 1994
Copyright © 1994 Elsevier Science Ltd
Printed in the USA. All rights reserved
0301-5629/94 $6.00 + .00

AUTHOR/SUBJECT INDEX

A

Ablation
acoustic properties of lesions generated with an ultrasound therapy system (Bush), 789
characterization of extracorporeal ablation of normal and tumor-bearing liver tissue by high intensity focused ultrasound (Sibille), 803
histological changes in rat liver tumours treated with high-intensity focused ultrasound (Chen), 67

Acoustic microscopy
quantification of ventricular remodeling in the tight-skin mouse cardiomyopathy with acoustic microscopy (Wong), 365

Acoustic speckle
compensation for the signal processing characteristics of ultrasound B-mode scanners in adaptive speckle reduction (Crawford), 469

Acoustic streaming
acoustic streaming generated by a focused Gaussian beam and finite amplitude tonebursts (Wu), 167

Acoustospectrography
correlations between acoustic and texture parameters from RF and B-mode liver echograms (Thijssen), 13
detection of diffuse liver disease by quantitative echography: dependence on *a priori* choice of parameters (Oosterveld), 21

Adamson, S. L., see Morrow, R. J.

Akselrod, S., see Mor-Avi, V.

Amiel, M., see Finet, G.

Anderson, T., see Li, S.

Arts, T. G. J., see Hoeks, A. P. G.

Aytac, S. K., see Özbek, S. S.

Adaptive processing
compensation for the signal processing characteristics of ultrasound B-mode scanners in adaptive speckle reduction (Crawford), 469

Albunex
a feasibility study on quantitating myocardial perfusion with Albunex®, an ultrasonic contrast agent (Wilson), 181
Doppler quantification of echo-contrast injections *in vivo* (Hartley), 269
quantification of transpulmonary echocontrast effects (de Jong), 279

Anastomoses
Doppler color flow images of iliofemoral graft end-to-side distal anastomotic models (Rittgers), 257

Angiography
intrarenal Doppler findings of upstream renal artery stenosis: a preliminary report (Özbek), 3

Angioplasty
intrarenal Doppler findings of upstream renal artery stenosis: a preliminary report (Özbek), 3

Angle-independent flow
a real time system for quantifying and displaying two-dimensional velocities using ultrasound (Bohs), 751

Anisotropy
quantification of ultrasonic anisotropy in normal myocardium with lateral gain compensation of two-dimensional integrated backscatter images (Recchia), 497

Anterior cerebral artery
Doppler colour flow mapping of fetal intracerebral arteries in the presence of central nervous system anomalies (Wladimiroff), 355

Aorta
aortic compliance measurements using Doppler ultrasound: *in vivo* biochemical correlates (Lehmann), 683
effects of pulsed ultrasound on the frog heart: I. Thresholds for changes in cardiac rhythm and aortic pressure (Dalecki), 385
effects of pulsed ultrasound on the frog heart: II. An investigation of heating as a potential mechanism (Dalecki), 391
experimentally induced changes in heart rate alter umbilicoplacental hemodynamics in fetal sheep (Morrow), 309

Arterial diameter
small arteries can be accurately studied *in vivo,* using high frequency ultrasound (Nielsen), 717

Artery
aortic compliance measurements using Doppler ultrasound: *in vivo* biochemical correlates (Lehmann), 683
Doppler colour flow mapping of fetal intracerebral arteries in the presence of central nervous system anomalies (Wladimiroff), 355
Doppler ultrasound spectral shape in the poststenotic velocity field (Hutchison), 649
experimentally induced changes in heart rate alter umbilicoplacental hemodynamics in fetal sheep (Morrow), 309
in vivo correlation of Doppler waveform analysis with arterial input impedance parameters (Downing), 549
intrarenal Doppler findings of upstream renal artery stenosis: a preliminary report (Özbek), 3
morphometry of intraluminal side-to-side differences in human basal cerebral arteries (Piepgras), 193

small arteries can be accurately studied *in vivo,* using high frequency ultrasound (Nielsen), 717
three-dimensional colour Doppler imaging (Picot), 95
transcranial colour coded sonography as an aid to measurement of blood flow velocity in the basal cerebral arteries (Martin), 711
transverse Doppler spectral analysis for a correct interpretation of flow sonograms (Tortoli), 115
volumetric arterial flow quantification using echo contrast. An *in vitro* comparison of three ultrasonic intensity methods: radio frequency, video and Doppler (Schwarz), 447

Artifacts
artifacts in intravascular ultrasound imaging: analyses and implications (Finet), 533
refraction in Doppler ultrasound (Li), 593L

Artificial heart valves
quantification of regurgitant flow through bileaflet heart valve prostheses: theoretical and *in vitro* studies (Cape), 461

Atherosclerosis
aortic compliance measurements using Doppler ultrasound: *in vivo* biochemical correlates (Lehmann), 683

Attenuation
acoustic properties of lesions generated with an ultrasound therapy system (Bush), 789
detection of diffuse liver disease by quantitative echography: dependence on *a priori* choice of parameters (Oosterveld), 21
estimation of *in situ* ultrasound exposure during obstetric examinations (Ramnarine), 319
thickness of tissues intervening between the transducer and fetus and models for fetal exposure calculations in transvaginal sonography (Kossoff), 59

Autocorrelation
comparison of the performance of the RF cross correlation and Doppler autocorrelation technique to estimate the mean velocity of simulated ultrasound signals (Hoeks), 727
range/velocity limitations for time-domain blood velocity estimation (Jensen), 741

B

B-mode imaging
a feasibility study on quantitating myocardial perfusion with Albunex®, an ultrasonic contrast agent (Wilson), 181
compensation for the signal processing characteristics of ultrasound B-mode scanners in adaptive speckle reduction (Crawford), 469
correlations between acoustic and texture parameters from RF and B-mode liver echograms (Thijssen), 13

Backscatter
a feasibility study on quantitating myocardial perfusion with Albunex®, an ultrasonic contrast agent (Wilson), 181
acoustic properties of lesions generated with an ultrasound therapy system (Bush), 789
detection of diffuse liver disease by quantitative echography: dependence on *a priori* choice of parameters (Oosterveld), 21
Doppler quantification of echo-contrast injections *in vivo* (Hartley), 269
effect of perfusion and blood content on ultrasonic backscattering of liver tissue (Kimitsuki), 39
on the Doppler signal from a steady flow asymmetrical stenosis model: effects of turbulence (Bascom), 197
quantification of transpulmonary echocontrast effects (de Jong), 279
quantification of ultrasonic anisotropy in normal myocardium with lateral gain compensation of two-dimensional integrated backscatter images (Recchia), 497
quantification of ventricular remodeling in the tight-skin mouse cardiomyopathy with acoustic microscopy (Wong), 365
quantitative echo contrast concentration measurement by Doppler sonography (Schwarz), 289
ultrasonic tissue characterization of experimental venous intimal hyperplasia (Parsons), 299
ultrasound myocardial integrated backscatter signal processing: frequency domain versus time domain (Rijsterborgh), 211

Bamber, J. C., see Bush, N. L.

Bamber, J. C., see Crawford, D. C.

Barnett, S. B., see Bosward, K. L.

Barnhart, J. L., see Wilson, B.

Basal cerebral artery
morphometry of intraluminal side-to-side differences in human basal cerebral arteries (Piepgras), 193
transcranial colour coded sonography as an aid to measurement of blood flow velocity in the basal cerebral arteries (Martin), 711

Bascom, P. A. J., Cobbold, R. S. C., Routh, H. F. and Johnston, K. W.: on the Doppler signal from a steady flow asymmetrical stenosis model: effects of turbulence, 197

Bashein, G., see Martin, R. W.

Beaune, J., see Finet, G.

Bell, D. S., see Crawford, D. C.

Bell, P. R. F., see Martin, P. J.

Bensted, J. P. M., see Chen, L.

Bezante, G. P., see Schwarz, K. Q.

Bhambhani, G. H., see Rittgers, S. E.

Bioeffects
a comparison of hemolytic and sonochemical activity of ultrasonic cavitation in a rotating tube (Miller), 83
acoustic properties of lesions generated with an ultrasound therapy system (Bush), 789

applications of lipid-coated microbubble ultrasonic contrast to tumor therapy (Simon), 123
biological effects of high energy shock waves in mouse skeletal muscle: correlation between ^{31}P magnetic resonance spectroscopic and microscopic alterations (Smits), 399
biological effects of laser-induced shock waves: structural and functional cell damage *in vitro* (Doukas), 137
cell density dependence of the ultrasonic degassing of fixed erythrocyte suspensions (Brayman), 243
characterization of extracorporeal ablation of normal and tumor-bearing liver tissue by high intensity focused ultrasound (Sibille), 803
effects of pulsed ultrasound on the frog heart: I. Thresholds for changes in cardiac rhythm and aortic pressure (Dalecki), 385
effects of pulsed ultrasound on the frog heart: II. An investigation of heating as a potential mechanism (Dalecki), 391
heating of guinea-pig fetal brain during exposure to pulsed ultrasound (Bosward), 415
histological changes in rat liver tumours treated with high-intensity focused ultrasound (Chen), 67
lysis of erythrocytes by exposure to CW ultrasound (Carstensen), 147
morphological effects of pulsed ultrasound in the lung (Penney), 127
temperature-dependent ultrasound color flow Doppler imaging in the study of a VX2 tumor in rabbits: preliminary findings (Shmulewitz), 221
the history of ultrasound techniques in ophthalmology (Thijssen), 599
the response of normal and malignant cells to ultrasound *in vitro* (Lejbkowicz), 75
timing of exposures in ultrasonic hemorrhage of murine lung (Raeman), 507
transient acoustic cavitation in gallstone fragmentation: a study of gallstones fragmented *in vivo* (Vakil), 331
ultrasonic gas body activation in *Elodea* leaves and the mechanical index (Miller), 343

Biometry

the history of ultrasound techniques in ophthalmology (Thijssen), 599

Bise, K., see Piepgras, A.

Bitton, Y., see Mor-Avi, V.

Blood

cell density dependence of the ultrasonic degassing of fixed erythrocyte suspensions (Brayman), 243
effect of perfusion and blood content on ultrasonic backscattering of liver tissue (Kimitsuki), 39
lysis of erythrocytes by exposure to CW ultrasound (Carstensen), 147

Blood flow

a feasibility study on quantitating myocardial perfusion with Albunex®, an ultrasonic contrast agent (Wilson), 181
a real time system for quantifying and displaying two-dimensional velocities using ultrasound (Bohs), 751
adaptive multipurpose probe fixation device for use on newborns (Michel), 581

Doppler color flow images of iliofemoral graft end-to-side distal anastomotic models (Rittgers), 257
Doppler colour flow mapping of fetal intracerebral arteries in the presence of central nervous system anomalies (Wladimiroff), 355
Doppler quantification of echo-contrast injections *in vivo* (Hartley), 269
Doppler ultrasound spectral shape in the poststenotic velocity field (Hutchison), 649
flow velocity waveforms in the ductus venosus, umbilical vein and inferior vena cava in normal human fetuses at 12–15 weeks of gestation (Huisman), 441
fractal concept and its analysis method for Doppler ultrasound signals (Wang), 661
in vivo correlation of Doppler waveform analysis with arterial input impedance parameters (Downing), 549
intrarenal Doppler findings of upstream renal artery stenosis: a preliminary report (Özbek), 3
myocardial regional blood flow: quantitative measurement by computer analysis of contrast enhanced echocardiographic images (Mor-Avi), 619
myocardial transit time of the echocardiographic contrast media (Mor-Avi), 635
on the Doppler signal from a steady flow asymmetrical stenosis model: effects of turbulence (Bascom), 197
quantification of regurgitant flow through bileaflet heart valve prostheses: theoretical and *in vitro* studies (Cape), 461
quantification of transpulmonary echocontrast effects (de Jong), 279
quantitative echo contrast concentration measurement by Doppler sonography (Schwarz), 289
temperature-dependent ultrasound color flow Doppler imaging in the study of a VX2 tumor in rabbits: preliminary findings (Shmulewitz), 221
three-dimensional colour Doppler imaging (Picot), 95
transcranial colour coded sonography as an aid to measurement of blood flow velocity in the basal cerebral arteries (Martin), 711
transverse Doppler spectral analysis for a correct interpretation of flow sonograms (Tortoli), 115
ultrasonic tissue characterization of experimental venous intimal hyperplasia (Parsons), 299
volumetric arterial flow quantification using echo contrast. An *in vitro* comparison of three ultrasonic intensity methods: radio frequency, video and Doppler (Schwarz), 447

Blood pressure
aortic compliance measurements using Doppler ultrasound: *in vivo* biochemical correlates (Lehmann), 683

Blood velocity
measurement of mean velocity during pulsatile flow using time-averaged maximum frequency of Doppler ultrasound waveforms (Li), 105
on the Doppler signal from a steady flow asymmetrical stenosis model: effects of turbulence (Bascom), 197
ultrasonic tissue characterization of experimental venous intimal hyperplasia (Parsons), 299

Bohs, L. N., Friemel, B. H., McDermott, B. A. and Trahey, G. E.: a real time system for quantifying and displaying two-dimensional velocities using ultrasound, 751

Bom, N., see Rijsterborgh, H.

Book reviews
Abdominal sonography: Sauerbrei, Nguyen and Nolan (Scharling), 425
Annual of genitourinary radiology and ultrasound: Pollack and Goldstein (Hissong), 425
Atlas of color-coded Doppler sonography: Fruhwald and Blackwell (Weill), 427
Doppler ultrasound in perinatal medicine: Pearce (Veille), 595
Intravascular ultrasound imaging: Cavaye and White (Strandness), 595
Introduction to vascular scanning: Ridgway (Burnham), 513
Techniques of venous imaging/Venous imaging technique: Talbot and Oliver (Daniel), 513
The search for Christian Doppler: Eden (Kremkau), 426
Output measurements for medical ultrasound: Preston (Harris), 426

Bosward, K. L., Barnett, S. B., Wood, A. K. W., Edwards, M. J. and Kossoff, G.: heating of guinea-pig fetal brain during exposure to pulsed ultrasound, 415

Brain
ultrasound-induced enhancement of ACh, AChE and GABA in fetal brain tissue of mouse (Suneetha), 411

Brands, P. J., see Hoeks, A. P. G.

Bravenec, J. S., see Hartley, C. J.

Brayman, A. A., see Carstensen, E. L.

Brayman, A. A. and Miller, M. W.: cell density dependence of the ultrasonic degassing of fixed erythrocyte suspensions, 243

Brezinka, Ch., Stijnen, Th., and Wladimiroff, J. W.: relationship between fetal pulmonary trunk and ductus arteriosus flow velocity waveforms in early normal pregnancy, 527

Bubbles
cell density dependence of the ultrasonic degassing of fixed erythrocyte suspensions (Brayman), 243
lysis of erythrocytes by exposure to CW ultrasound (Carstensen), 147
the effect of gas bubbles on the production of ultrasound hyperthermia at 0.75 MHz: a phantom study (Watmough), 231
ultrasonic gas body activation in *Elodea* leaves and the mechanical index (Miller), 343

Bulic, M., see Podobnik, M.

Bull, S. B., see Morrow, R. J.

Bush, N. L., Rivens, I., ter Haar, G. R. and Bamber, J. C.: acoustic properties of lesions generated with an ultrasound therapy system, 789

C

Cape, E. G., Nanda, N. C. and Yoganathan, A. P.: quantification of regurgitant flow through bileaflet heart valve prostheses: theoretical and *in vitro* studies, 461

Can, A., see Parsons, R. E.

Canine muscle
non-Rayleigh first-order statistics of ultrasonic backscatter from normal myocardium (Clifford), 487

Cardiac myofibers
quantification of ultrasonic anisotropy in normal myocardium with lateral gain compensation of two-dimensional integrated backscatter images (Recchia), 497

Cardiac rhythm
effects of pulsed ultrasound on the frog heart: I. Thresholds for changes in cardiac rhythm and aortic pressure (Dalecki), 385
effects of pulsed ultrasound on the frog heart: II. An investigation of heating as a potential mechanism (Dalecki), 391

Cardiography
Doppler quantification of echo-contrast injections *in vivo* (Hartley), 269
methodology for three-dimensional reconstruction of the left ventricle from transesophageal echocardiograms (Martin), 27
myocardial regional blood flow: quantitative measurement by computer analysis of contrast enhanced echocardiographic images (Mor-Avi), 619
myocardial transit time of the echocardiographic contrast media (Mor-Avi), 635
quantification of regurgitant flow through bileaflet heart valve prostheses: theoretical and *in vitro* studies (Cape), 461
quantification of transpulmonary echocontrast effects (de Jong), 279
quantification of ventricular remodeling in the tight-skin mouse cardiomyopathy with acoustic microscopy (Wong), 365
relationship between fetal pulmonary trunk and ductus arteriosus flow velocity waveforms in early normal pregnancy (Brezinka), 527

Cardiomyopathy
quantification of ventricular remodeling in the tight-skin mouse cardiomyopathy with acoustic microscopy (Wong), 365

Carotid
three-dimensional colour Doppler imaging (Picot), 95
transverse Doppler spectral analysis for a correct interpretation of flow sonograms (Tortoli), 115

Carpal tunnel syndrome
ultrasound myography: application in nerve conduction velocity assessment and muscle cooling (Journée), 561

Carstensen, E. L., Kelly, P., Church, C. C., Brayman, A. A., Child, S. Z., Raeman, C. H. and Schery, L.: lysis of erythrocytes by exposure to CW ultrasound, 147

Carstensen, E. L., see Dalecki, D.

Carstensen, E. L., see Penney, D. P.

Carstensen, E. L., see Raeman, C. H.

Case, C. Q., see Dillon, E. H.

Cathignol, D., see Sibille, A.

Cavitation

a comparison of hemolytic and sonochemical activity of ultrasonic cavitation in a rotating tube (Miller), 83

applications of lipid-coated microbubble ultrasonic contrast to tumor therapy (Simon), 123

biological effects of high energy shock waves in mouse skeletal muscle: correlation between ^{31}P magnetic resonance spectroscopic and microscopic alterations (Smits), 399

biological effects of laser-induced shock waves: structural and functional cell damage *in vitro* (Doukas), 137

cell density dependence of the ultrasonic degassing of fixed erythrocyte suspensions (Brayman), 243

characterization of extracorporeal ablation of normal and tumor-bearing liver tissue by high intensity focused ultrasound (Sibille), 803

lysis of erythrocytes by exposure to CW ultrasound (Carstensen), 147

the effect of gas bubbles on the production of ultrasound hyperthermia at 0.75 MHz: a phantom study (Watmough), 231

timing of exposures in ultrasonic hemorrhage of murine lung (Raeman), 507

transient acoustic cavitation in gallstone fragmentation: a study of gallstones fragmented *in vivo* (Vakil), 331

ultrasonic gas body activation in *Elodea* leaves and the mechanical index (Miller), 343

Cell lysis

a comparison of hemolytic and sonochemical activity of ultrasonic cavitation in a rotating tube (Miller), 83

cell density dependence of the ultrasonic degassing of fixed erythrocyte suspensions (Brayman), 243

lysis of erythrocytes by exposure to CW ultrasound (Carstensen), 147

morphological effects of pulsed ultrasound in the lung (Penney), 127

Cells

a comparison of hemolytic and sonochemical activity of ultrasonic cavitation in a rotating tube (Miller), 83

applications of lipid-coated microbubble ultrasonic contrast to tumor therapy (Simon), 123

biological effects of high energy shock waves in mouse skeletal muscle: correlation between ^{31}P magnetic resonance spectroscopic and microscopic alterations (Smits), 399

biological effects of laser-induced shock waves: structural and functional cell damage *in vitro* (Doukas), 137

cell density dependence of the ultrasonic degassing of fixed erythrocyte suspensions (Brayman), 243

histological changes in rat liver tumours treated with high-intensity focused ultrasound (Chen), 67

lysis of erythrocytes by exposure to CW ultrasound (Carstensen), 147
morphological effects of pulsed ultrasound in the lung (Penney), 127
the response of normal and malignant cells to ultrasound *in vitro* (Lejbkowicz), 75

Central nervous system pathology
Doppler colour flow mapping of fetal intracerebral arteries in the presence of central nervous system anomalies (Wladimiroff), 355

Cerebral arteries
Doppler colour flow mapping of fetal intracerebral arteries in the presence of central nervous system anomalies (Wladimiroff), 355
morphometry of intraluminal side-to-side differences in human basal cerebral arteries (Piepgras), 193
transcranial colour coded sonography as an aid to measurement of blood flow velocity in the basal cerebral arteries (Martin), 711

Cerebral flow
adaptive multipurpose probe fixation device for use on newborns (Michel), 581
Doppler colour flow mapping of fetal intracerebral arteries in the presence of central nervous system anomalies (Wladimiroff), 355

Chapelon, J.-Y., see Sibille, A.

Cheirif, J., see Hartley, C. J.

Chen, L., Rivens, I., ter Haar, G., Riddler, S., Hill, C. R. and Bensted, J. P. M.: histological changes in rat liver tumours treated with high-intensity focused ultrasound, 67

Chen, X., see Schwarz, K. Q.

Child, S. Z., see Carstensen, E. L.

Child, S. Z., see Penney, D. P.

Child, S. Z., see Raeman, C. H.

Choshniak, I., see Mor-Avi, V.

Church, C. C., see Carstensen, E. L.

Ciglar, S., see Podobnik, M.

Clifford, L., Fitzgerald, P. and James, D.: non-Rayleigh first-order statistics of ultrasonic backscatter from normal myocardium, 487

Cobbold, R. S. C., see Bascom, P. A. J.

Coldwell, D., see Shmulewitz, A.

Collier, K. R., see Hartley, C. J.

Color flow Doppler
a real time system for quantifying and displaying two-dimensional velocities using ultrasound (Bohs), 751
comparison of various agents in contrast enhancement of color Doppler flow images: an *in vitro* study (Fan), 45
Doppler color flow images of iliofemoral graft end-to-side distal anastomotic models (Rittgers), 257
Doppler colour flow mapping of fetal intracerebral arteries in the presence of central nervous system anomalies (Wladimiroff), 355

endovaginal pulsed and color Doppler in first-trimester pregnancy (Dillon), 517
intrarenal Doppler findings of upstream renal artery stenosis: a preliminary report (Özbek), 3
preoperative diagnosis of primary fallopian tube carcinoma by transvaginal ultrasound, cytological finding and CA-125 (Podobnik), 587
temperature-dependent ultrasound color flow Doppler imaging in the study of a VX2 tumor in rabbits: preliminary findings (Shmulewitz), 221
three-dimensional colour Doppler imaging (Picot), 95
transcranial colour coded sonography as an aid to measurement of blood flow velocity in the basal cerebral arteries (Martin), 711

Color vector display
a real time system for quantifying and displaying two-dimensional velocities using ultrasound (Bohs), 751

Compliance
aortic compliance measurements using Doppler ultrasound: *in vivo* biochemical correlates (Lehmann), 683

Computer algorithm
methodology for three-dimensional reconstruction of the left ventricle from transesophageal echocardiograms (Martin), 27

Contrast
a feasibility study on quantitating myocardial perfusion with Albunex®, an ultrasonic contrast agent (Wilson), 181
applications of lipid-coated microbubble ultrasonic contrast to tumor therapy (Simon), 123
comparison of various agents in contrast enhancement of color Doppler flow images: an *in vitro* study (Fan), 45
Doppler quantification of echo-contrast injections *in vivo* (Hartley), 269
myocardial regional blood flow: quantitative measurement by computer analysis of contrast enhanced echocardiographic images (Mor-Avi), 619
myocardial transit time of the echocardiographic contrast media (Mor-Avi), 635
quantification of transpulmonary echocontrast effects (de Jong), 279
quantitative echo contrast concentration measurement by Doppler sonography (Schwarz), 289
second harmonic ultrasonic blood perfusion measurement (Schrope), 567
volumetric arterial flow quantification using echo contrast. An *in vitro* comparison of three ultrasonic intensity methods: radio frequency, video and Doppler (Schwarz), 447

Cracks
transient acoustic cavitation in gallstone fragmentation: a study of gallstones fragmented *in vivo* (Vakil), 331

Crawford, D. C., Bell, D. S. and Bamber, J. C.: compensation for the signal processing characteristics of ultrasound B-mode scanners in adaptive speckle reduction, 469

Cross-correlation
comparison of the performance of the RF cross correlation and Doppler

autocorrelation technique to estimate the mean velocity of simulated ultrasound signals (Hoeks), 727
correction of phase aberrations for sectored annular array ultrasound transducers (Gambetti), 763
range/velocity limitations for time-domain blood velocity estimation (Jensen), 741

Crowley, R. J., see Finet, G.

Czuwala, P. J., see Fan, P.

D

Dalecki, D., Keller, B. B., Raeman, C. H. and Carstensen, E. L.: effects of pulsed ultrasound on the frog heart: I. Thresholds for changes in cardiac rhythm and aortic pressure, 385

Dalecki, D., Raeman, C. H. and Carstensen, E. L.: effects of pulsed ultrasound on the frog heart: II. An investigation of heating as a potential mechanism, 391

Damianou, C. and Hynynen, K.: focal spacing and near-field heating during pulsed high temperature ultrasound therapy, 777

Damianou, C., see Hynynen, K.

Darkazanli, A., see Hynynen, K.

David, D., see Mor-Avi, V.

Debruyne, F. M. J., see Smits, G. A. H. J.

Diabetes
aortic compliance measurements using Doppler ultrasound: *in vivo* biochemical correlates (Lehmann), 683

Diameter measurement
small arteries can be accurately studied *in vivo,* using high frequency ultrasound (Nielsen), 717

Diffuse liver disease
detection of diffuse liver disease by quantitative echography: dependence on *a priori* choice of parameters (Oosterveld), 21

Dillon, E. H., Case, C. Q., Ramos, I. M., Holland, C. K. and Taylor, K. J. W.: endovaginal pulsed and color Doppler in first-trimester pregnancy, 517

Discriminant analysis
detection of diffuse liver disease by quantitative echography: dependence on *a priori* choice of parameters (Oosterveld), 21

Distensibility
aortic compliance measurements using Doppler ultrasound: *in vivo* biochemical correlates (Lehmann), 683

Dog
non-Rayleigh first-order statistics of ultrasonic backscatter from normal myocardium (Clifford), 487

quantification of ultrasonic anisotropy in normal myocardium with lateral gain compensation of two-dimensional integrated backscatter images (Recchia), 497

Doppler
a feasibility study on quantitating myocardial perfusion with Albunex®, an ultrasonic contrast agent (Wilson), 181
a real time system for quantifying and displaying two-dimensional velocities using ultrasound (Bohs), 751
adaptive multipurpose probe fixation device for use on newborns (Michel), 581
comparison of the performance of the RF cross correlation and Doppler autocorrelation technique to estimate the mean velocity of simulated ultrasound signals (Hoeks), 727
comparison of various agents in contrast enhancement of color Doppler flow images: an *in vitro* study (Fan), 45
Doppler color flow images of iliofemoral graft end-to-side distal anastomotic models (Rittgers), 257
Doppler colour flow mapping of fetal intracerebral arteries in the presence of central nervous system anomalies (Wladimiroff), 355
Doppler quantification of echo-contrast injections *in vivo* (Hartley), 269
Doppler ultrasound spectral shape in the poststenotic velocity field (Hutchison), 649
endovaginal pulsed and color Doppler in first-trimester pregnancy (Dillon), 517
flow velocity waveforms in the ductus venosus, umbilical vein and inferior vena cava in normal human fetuses at 12–15 weeks of gestation (Huisman), 441
fractal concept and its analysis method for Doppler ultrasound signals (Wang), 661
in vivo correlation of Doppler waveform analysis with arterial input impedance parameters (Downing), 549
intrarenal Doppler findings of upstream renal artery stenosis: a preliminary report (Özbek), 3
measurement of mean velocity during pulsatile flow using time-averaged maximum frequency of Doppler ultrasound waveforms (Li), 105
myocardial regional blood flow: quantitative measurement by computer analysis of contrast enhanced echocardiographic images (Mor-Avi), 619
myocardial transit time of the echocardiographic contrast media (Mor-Avi), 635
nonlinear propagation in Doppler ultrasound (Li), 359
on the Doppler signal from a steady flow asymmetrical stenosis model: effects of turbulence (Bascom), 197
preoperative diagnosis of primary fallopian tube carcinoma by transvaginal ultrasound, cytological finding and CA-125 (Podobnik), 587
quantification of regurgitant flow through bileaflet heart valve prostheses: theoretical and *in vitro* studies (Cape), 461
quantification of transpulmonary echocontrast effects (de Jong), 279
quantitative echo contrast concentration measurement by Doppler sonography (Schwarz), 289
refraction in Doppler ultrasound (Li), 593L
relationship between fetal pulmonary trunk and ductus arteriosus flow velocity waveforms in early normal pregnancy (Brezinka), 527

second harmonic ultrasonic blood perfusion measurement (Schrope), 567
temperature-dependent ultrasound color flow Doppler imaging in the study of a VX2 tumor in rabbits: preliminary findings (Shmulewitz), 221
three-dimensional colour Doppler imaging (Picot), 95
transcranial colour coded sonography as an aid to measurement of blood flow velocity in the basal cerebral arteries (Martin), 711
transverse Doppler spectral analysis for a correct interpretation of flow sonograms (Tortoli), 115
ultrasonic tissue characterization of experimental venous intimal hyperplasia (Parsons), 299
ultrasound myography: application in nerve conduction velocity assessment and muscle cooling (Journée), 561
volumetric arterial flow quantification using echo contrast. An *in vitro* comparison of three ultrasonic intensity methods: radio frequency, video and Doppler (Schwarz), 447

Doppler indices
endovaginal pulsed and color Doppler in first-trimester pregnancy (Dillon), 517
in vivo correlation of Doppler waveform analysis with arterial input impedance parameters (Downing), 549
intrarenal Doppler findings of upstream renal artery stenosis: a preliminary report (Özbek), 3
on the Doppler signal from a steady flow asymmetrical stenosis model: effects of turbulence (Bascom), 197
ultrasonic tissue characterization of experimental venous intimal hyperplasia (Parsons), 299

Dosimetry
a comparison of hemolytic and sonochemical activity of ultrasonic cavitation in a rotating tube (Miller), 83
acoustic properties of lesions generated with an ultrasound therapy system (Bush), 789
characterization of extracorporeal ablation of normal and tumor-bearing liver tissue by high intensity focused ultrasound (Sibille), 803
estimation of *in situ* ultrasound exposure during obstetric examinations (Ramnarine), 319
lysis of erythrocytes by exposure to CW ultrasound (Carstensen), 147
ultrasonic gas body activation in *Elodea* leaves and the mechanical index (Miller), 343

Doukas, A. G., McAuliffe, D. J. and Flotte, T. J.: biological effects of laser-induced shock waves: structural and functional cell damage *in vitro*, 137

Downing, G. J., Maulik, D., Phillips, C. and Kadado, T. R.: *in vivo* correlation of Doppler waveform analysis with arterial input impedance parameters, 549

D'Arrigo, J. S., see Simon, R. H.

Du, G., see Wu, J.

Ductus arteriosus
relationship between fetal pulmonary trunk and ductus arteriosus flow velocity waveforms in early normal pregnancy (Brezinka), 527

Ductus venosus
flow velocity waveforms in the ductus venosus, umbilical vein and inferior vena cava in normal human fetuses at 12–15 weeks of gestation (Huisman), 441

E

Edwards, M. J., see Bosward, K. L.

Erden, M. I., see Özbek, S. S.

Evans, D. H., see Martin, P. J.

Everbach, E. C., see Vakil, N.

Echocardiography
Doppler quantification of echo-contrast injections *in vivo* (Hartley), 269
methodology for three-dimensional reconstruction of the left ventricle from transesophageal echocardiograms (Martin), 27
myocardial regional blood flow: quantitative measurement by computer analysis of contrast enhanced echocardiographic images (Mor-Avi), 619
myocardial transit time of the echocardiographic contrast media (Mor-Avi), 635
quantification of regurgitant flow through bileaflet heart valve prostheses: theoretical and *in vitro* studies (Cape), 461
quantification of transpulmonary echocontrast effects (de Jong), 279
relationship between fetal pulmonary trunk and ductus arteriosus flow velocity waveforms in early normal pregnancy (Brezinka), 527
ultrasound myocardial integrated backscatter signal processing: frequency domain versus time domain (Rijsterborgh), 211

Echogram
correlations between acoustic and texture parameters from RF and B-mode liver echograms (Thijssen), 13

El Fadil, F. A., see Sibille, A.

Elasticity
aortic compliance measurements using Doppler ultrasound: *in vivo* biochemical correlates (Lehmann), 683

Electromyography
ultrasound myography: application in nerve conduction velocity assessment and muscle cooling (Journée), 561

Electron microscopy
biological effects of high energy shock waves in mouse skeletal muscle: correlation between ^{31}P magnetic resonance spectroscopic and microscopic alterations (Smits), 399
biological effects of laser-induced shock waves: structural and functional cell damage *in vitro* (Doukas), 137
morphological effects of pulsed ultrasound in the lung (Penney), 127
transient acoustic cavitation in gallstone fragmentation: a study of gallstones fragmented *in vivo* (Vakil), 331

Elodea
ultrasonic gas body activation in *Elodea* leaves and the mechanical index (Miller), 343

Erythrocytes
cell density dependence of the ultrasonic degassing of fixed erythrocyte suspensions (Brayman), 243
lysis of erythrocytes by exposure to CW ultrasound (Carstensen), 147

ESWL
biological effects of high energy shock waves in mouse skeletal muscle: correlation between ^{31}P magnetic resonance spectroscopic and microscopic alterations (Smits), 399
morphological effects of pulsed ultrasound in the lung (Penney), 127
transient acoustic cavitation in gallstone fragmentation: a study of gallstones fragmented *in vivo* (Vakil), 331

Exposure
acoustic properties of lesions generated with an ultrasound therapy system (Bush), 789
characterization of extracorporeal ablation of normal and tumor-bearing liver tissue by high intensity focused ultrasound (Sibille), 803
estimation of *in situ* ultrasound exposure during obstetric examinations (Ramnarine), 319
focal spacing and near-field heating during pulsed high temperature ultrasound therapy (Damianou), 777
thickness of tissues intervening between the transducer and fetus and models for fetal exposure calculations in transvaginal sonography (Kossoff), 59
ultrasonic gas body activation in *Elodea* leaves and the mechanical index (Miller), 343

F

Fan, P., Czuwala, P. J., Nanda, N. C., Rosenthal, S. M. and Yoganathan, A.: comparison of various agents in contrast enhancement of color Doppler flow images: an *in vitro* study, 45

Filipczyński, L., Kujawska, T. and Wojcik, J.: temperature elevation in focused Gaussian ultrasonic beams at various insonation times, 667

Finet, G., Maurincomme, E., Tabib, A., Crowley, R. J., Magnin, I., Roriz, R., Beaune, J. and Amiel, M.: artifacts in intravascular ultrasound imaging: analyses and implications, 533

Feleppa, E. J., see Kimitsuki, H.

Feleppa, E. J., see Parsons, R. E.

Fenster, A., see Picot, P. A.

Fitzgerald, P., see Clifford, L.

Flotte, T. J., see Doukas, A. G.

Foster, F. S., see Gambetti, C.

Foster, F. S., see McKinley, C. A.

Friemel, B. H., see Bohs, L. N.

Fetal blood flow
flow velocity waveforms in the ductus venosus, umbilical vein and inferior vena cava in normal human fetuses at 12–15 weeks of gestation (Huisman), 441
relationship between fetal pulmonary trunk and ductus arteriosus flow velocity waveforms in early normal pregnancy (Brezinka), 527
ultrasonic tissue characterization of experimental venous intimal hyperplasia (Parsons), 299

Fetal circulation
flow velocity waveforms in the ductus venosus, umbilical vein and inferior vena cava in normal human fetuses at 12–15 weeks of gestation (Huisman), 441
relationship between fetal pulmonary trunk and ductus arteriosus flow velocity waveforms in early normal pregnancy (Brezinka), 527
ultrasonic tissue characterization of experimental venous intimal hyperplasia (Parsons), 299

Fetus
estimation of *in situ* ultrasound exposure during obstetric examinations (Ramnarine), 319
thickness of tissues intervening between the transducer and fetus and models for fetal exposure calculations in transvaginal sonography (Kossoff), 59
ultrasound-induced enhancement of ACh, AChE and GABA in fetal brain tissue of mouse (Suneetha), 411

Fibrosarcoma
histological changes in rat liver tumours treated with high-intensity focused ultrasound (Chen), 67

Filtering
compensation for the signal processing characteristics of ultrasound B-mode scanners in adaptive speckle reduction (Crawford), 469

Flow
a feasibility study on quantitating myocardial perfusion with Albunex®, an ultrasonic contrast agent (Wilson), 181
a real time system for quantifying and displaying two-dimensional velocities using ultrasound (Bohs), 751
adaptive multipurpose probe fixation device for use on newborns (Michel), 581
comparison of various agents in contrast enhancement of color Doppler flow images: an *in vitro* study (Fan), 45
Doppler color flow images of iliofemoral graft end-to-side distal anastomotic models (Rittgers), 257
Doppler colour flow mapping of fetal intracerebral arteries in the presence of central nervous system anomalies (Wladimiroff), 355
Doppler quantification of echo-contrast injections *in vivo* (Hartley), 269
Doppler ultrasound spectral shape in the poststenotic velocity field (Hutchison), 649
flow velocity waveforms in the ductus venosus, umbilical vein and inferior vena cava in normal human fetuses at 12–15 weeks of gestation (Huisman), 441

fractal concept and its analysis method for Doppler ultrasound signals (Wang), 661
in vivo correlation of Doppler waveform analysis with arterial input impedance parameters (Downing), 549
intrarenal Doppler findings of upstream renal artery stenosis: a preliminary report (Özbek), 3
measurement of mean velocity during pulsatile flow using time-averaged maximum frequency of Doppler ultrasound waveforms (Li), 105
myocardial regional blood flow: quantitative measurement by computer analysis of contrast enhanced echocardiographic images (Mor-Avi), 619
myocardial transit time of the echocardiographic contrast media (Mor-Avi), 635
on the Doppler signal from a steady flow asymmetrical stenosis model: effects of turbulence (Bascom), 197
quantification of regurgitant flow through bileaflet heart valve prostheses: theoretical and *in vitro* studies (Cape), 461
quantification of transpulmonary echocontrast effects (de Jong), 279
quantitative echo contrast concentration measurement by Doppler sonography (Schwarz), 289
temperature-dependent ultrasound color flow Doppler imaging in the study of a VX2 tumor in rabbits: preliminary findings (Shmulewitz), 221
three-dimensional colour Doppler imaging (Picot), 95
transcranial colour coded sonography as an aid to measurement of blood flow velocity in the basal cerebral arteries (Martin), 711
transverse Doppler spectral analysis for a correct interpretation of flow sonograms (Tortoli), 115
ultrasonic tissue characterization of experimental venous intimal hyperplasia (Parsons), 299
volumetric arterial flow quantification using echo contrast. An *in vitro* comparison of three ultrasonic intensity methods: radio frequency, video and Doppler (Schwarz), 447

Flow phantom
comparison of various agents in contrast enhancement of color Doppler flow images: an *in vitro* study (Fan), 45
Doppler color flow images of iliofemoral graft end-to-side distal anastomotic models (Rittgers), 257
measurement of mean velocity during pulsatile flow using time-averaged maximum frequency of Doppler ultrasound waveforms (Li), 105
volumetric arterial flow quantification using echo contrast. An *in vitro* comparison of three ultrasonic intensity methods: radio frequency, video and Doppler (Schwarz), 447

Flow profile
Doppler color flow images of iliofemoral graft end-to-side distal anastomotic models (Rittgers), 257
Doppler ultrasound spectral shape in the poststenotic velocity field (Hutchison), 649
on the Doppler signal from a steady flow asymmetrical stenosis model: effects of turbulence (Bascom), 197

Flow separation
Doppler color flow images of iliofemoral graft end-to-side distal anastomotic models (Rittgers), 257

Doppler ultrasound spectral shape in the poststenotic velocity field (Hutchison), 649

Flow velocity waveform
measurement of mean velocity during pulsatile flow using time-averaged maximum frequency of Doppler ultrasound waveforms (Li), 105
relationship between fetal pulmonary trunk and ductus arteriosus flow velocity waveforms in early normal pregnancy (Brezinka), 527

Fluid dynamics
Doppler color flow images of iliofemoral graft end-to-side distal anastomotic models (Rittgers), 257
quantification of regurgitant flow through bileaflet heart valve prostheses: theoretical and *in vitro* studies (Cape), 461
volumetric arterial flow quantification using echo contrast. An *in vitro* comparison of three ultrasonic intensity methods: radio frequency, video and Doppler (Schwarz), 447

Focused transducers
acoustic properties of lesions generated with an ultrasound therapy system (Bush), 789
characterization of extracorporeal ablation of normal and tumor-bearing liver tissue by high intensity focused ultrasound (Sibille), 803
histological changes in rat liver tumours treated with high-intensity focused ultrasound (Chen), 67

Fontanelle
adaptive multipurpose probe fixation device for use on newborns (Michel), 581

Fractals
fractal concept and its analysis method for Doppler ultrasound signals (Wang), 661

Free radicals
a comparison of hemolytic and sonochemical activity of ultrasonic cavitation in a rotating tube (Miller), 83

Frequency domain
ultrasound myocardial integrated backscatter signal processing: frequency domain versus time domain (Rijsterborgh), 211

Frog heart
effects of pulsed ultrasound on the frog heart: I. Thresholds for changes in cardiac rhythm and aortic pressure (Dalecki), 385
effects of pulsed ultrasound on the frog heart: II. An investigation of heating as a potential mechanism (Dalecki), 391

G

Gallstones
in vitro evaluation of gallstone dissolution with methyl-tert-butyl ether and ultrasound energy (McKinley), 375
transient acoustic cavitation in gallstone fragmentation: a study of gallstones fragmented *in vivo* (Vakil), 331

Gambetti, C. and Foster, F. S.: correction of phase aberrations for sectored annular array ultrasound transducers, 763

Garrett, W. J., see Kossoff, G.

Gas body activation
Ultrasonic gas body activation in *Elodea* leaves and the mechanical index (Miller), 343

Gas bubbles
the effect of gas bubbles on the production of ultrasound hyperthermia at 0.75 MHz: a phantom study (Watmough), 231

Gaussian beams
acoustic streaming generated by a focused Gaussian beam and finite amplitude tonebursts (Wu), 167
temperature elevation in focused Gaussian ultrasonic beams at various insonation times (Filipczyński), 667

Ghezzi, F., see Watmough, D. J.

Golub, R. M., see Kimitsuki, H.

Golub, R. M., see Parsons, R. E.

Gosling, R. G., see Lehmann, E. D.

Graft anastomoses
Doppler color flow images of iliofemoral graft end-to-side distal anastomotic models (Rittgers), 257

Griffiths, K. A., see Kossoff, G.

Growth factors
aortic compliance measurements using Doppler ultrasound: *in vivo* biochemical correlates (Lehmann), 683

Guidi, G., see Tortoli, P.

Guinea pig
heating of guinea-pig fetal brain during exposure to pulsed ultrasound (Bosward), 415

H

ter Haar, G. R., see Bush, N. L.

ter Haar, G. R., see Chen, L.

Haemodynamics
In vivo correlation of Doppler waveform analysis with arterial input impedance parameters (Downing), 549
ultrasonic tissue characterization of experimental venous intimal hyperplasia (Parsons), 299

Hartley, C. J., Cheirif, J., Collier, K. R., Bravenec, J. S. and Mickelson, J. K.: Doppler quantification of echo-contrast injections *in vivo*, 269

Hartman, P. C., see Oosterveld, B. J.

Hartman, P. C., see Thijssen, J. M.

Hartman-Raeman, C., see Penney, D. P.

Heart valves
quantification of regurgitant flow through bileaflet heart valve prostheses: theoretical and *in vitro* studies (Cape), 461

Heating
applications of lipid-coated microbubble ultrasonic contrast to tumor therapy (Simon), 123
effects of pulsed ultrasound on the frog heart: II. An investigation of heating as a potential mechanism (Dalecki), 391
heating of guinea-pig fetal brain during exposure to pulsed ultrasound (Bosward), 415
histological changes in rat liver tumours treated with high-intensity focused ultrasound (Chen), 67
temperature-dependent ultrasound color flow Doppler imaging in the study of a VX2 tumor in rabbits: preliminary findings (Shmulewitz), 221
the effect of gas bubbles on the production of ultrasound hyperthermia at 0.75 MHz: a phantom study (Watmough), 231

Heerschap, A., see Smits, G. A. H. J.

Hematocrit
on the Doppler signal from a steady flow asymmetrical stenosis model: effects of turbulence (Bascom), 197

Hemorrhage
morphological effects of pulsed ultrasound in the lung (Penney), 127

Henry, L., see Sibille, A.

Hete, B., see Wilson, B.

Heydanus, R., see Wladimiroff, J. W.

High frequency imaging
small arteries can be accurately studied *in vivo,* using high frequency ultrasound (Nielsen), 717

High resolution
small arteries can be accurately studied *in vivo,* using high frequency ultrasound (Nielsen), 717

Hill, C. R., see Chen, L.

Histological changes
acoustic properties of lesions generated with an ultrasound therapy system (Bush), 789
biological effects of high energy shock waves in mouse skeletal muscle: correlation between ^{31}P magnetic resonance spectroscopic and microscopic alterations (Smits), 399
biological effects of laser-induced shock waves: structural and functional cell damage *in vitro* (Doukas), 137
characterization of extracorporeal ablation of normal and tumor-bearing liver tissue by high intensity focused ultrasound (Sibille), 803
histological changes in rat liver tumours treated with high-intensity focused ultrasound (Chen), 67
morphological effects of pulsed ultrasound in the lung (Penney), 127
ultrasonic tissue characterization of experimental venous intimal hyperplasia (Parsons), 299

History
the history of ultrasound techniques in ophthalmology (Thijssen), 599

Ho, C.-S., see McKinley, C. A.

Ho, S.-Y., see Simon, R. H.

Hoeks, A. P. G., Arts, T. G. J., Brands, P. J. and Reneman, R. S.: comparison of the performance of the RF cross correlation and Doppler autocorrelation technique to estimate the mean velocity of simulated ultrasound signals, 727

Holland, C. K., see Dillon, E. H.

Hopkins, K. D., see Lehmann, E. D.

Hoskins, P. R., see Li, S.

Huisman, T. W. A., Stewart, P. A., Wladimiroff, J. W. and Stijnen, T.: flow velocity waveforms in the ductos venosus, umbilical vein and inferior vena cava in normal human fetuses at 12–15 weeks of gestation, 441

Hunt, J. W., see McKinley, C. A.

Hutchison, K. J.: Doppler ultrasound spectral shape in the poststenotic velocity field, 649

Hydrogen peroxide
a comparison of hemolytic and sonochemical activity of ultrasonic cavitation in a rotating tube (Miller), 83

Hynynen, K., Damianou, C., Darkazanli, A., Unger, E. and Schenck, J. F.: the feasibility of using MRI to monitor and guide noninvasive surgery, 91L

Hynynen, K., see Damianou, C.

Hyperthermia
acoustic properties of lesions generated with an ultrasound therapy system (Bush), 789
applications of lipid-coated microbubble ultrasonic contrast to tumor therapy (Simon), 123
focal spacing and near-field heating during pulsed high temperature ultrasound therapy (Damianou), 777
histological changes in rat liver tumours treated with high-intensity focused ultrasound (Chen), 67
temperature-dependent ultrasound color flow Doppler imaging in the study of a VX2 tumor in rabbits: preliminary findings (Shmulewitz), 221
the effect of gas bubbles on the production of ultrasound hyperthermia at 0.75 MHz: a phantom study (Watmough), 231

I

Image processing
compensation for the signal processing characteristics of ultrasound B-mode scanners in adaptive speckle reduction (Crawford), 469
relationship between fetal pulmonary trunk and ductus arteriosus flow velocity waveforms in early normal pregnancy (Brezinka), 527

Imaging
acoustic properties of lesions generated with an ultrasound therapy system (Bush), 789

correction of phase aberrations for sectored annular array ultrasound transducers (Gambetti), 763
quantification of ultrasonic anisotropy in normal myocardium with lateral gain compensation of two-dimensional integrated backscatter images (Recchia), 497
relationship between fetal pulmonary trunk and ductus arteriosus flow velocity waveforms in early normal pregnancy (Brezinka), 527
three-dimensional colour Doppler imaging (Picot), 95

Impedance
in vivo correlation of Doppler waveform analysis with arterial input impedance parameters (Downing), 549

In vitro *irradiation*
a comparison of hemolytic and sonochemical activity of ultrasonic cavitation in a rotating tube (Miller), 83
acoustic properties of lesions generated with an ultrasound therapy system (Bush), 789
biological effects of laser-induced shock waves: structural and functional cell damage *in vitro* (Doukas), 137
cell density dependence of the ultrasonic degassing of fixed erythrocyte suspensions (Brayman), 243
lysis of erythrocytes by exposure to CW ultrasound (Carstensen), 147
temperature elevation in focused Gaussian ultrasonic beams at various insonation times (Filipczyński), 667
the effect of gas bubbles on the production of ultrasound hyperthermia at 0.75 MHz: a phantom study (Watmough), 231
the response of normal and malignant cells to ultrasound *in vitro* (Lejbkowicz), 75
ultrasonic gas body activation in *Elodea* leaves and the mechanical index (Miller), 343

In vivo *irradiation*
applications of lipid-coated microbubble ultrasonic contrast to tumor therapy (Simon), 123
biological effects of high energy shock waves in mouse skeletal muscle: correlation between ^{31}P magnetic resonance spectroscopic and microscopic alterations (Smits), 399
characterization of extracorporeal ablation of normal and tumor-bearing liver tissue by high intensity focused ultrasound (Sibille), 803
effects of pulsed ultrasound on the frog heart: I. Thresholds for changes in cardiac rhythm and aortic pressure (Dalecki), 385
effects of pulsed ultrasound on the frog heart: II. An investigation of heating as a potential mechanism (Dalecki), 391
focal spacing and near-field heating during pulsed high temperature ultrasound therapy (Damianou), 777
heating of guinea-pig fetal brain during exposure to pulsed ultrasound (Bosward), 415
histological changes in rat liver tumours treated with high-intensity focused ultrasound (Chen), 67
in vitro evaluation of gallstone dissolution with methyl-tert-butyl ether and ultrasound energy (McKinley), 375
morphological effects of pulsed ultrasound in the lung (Penney), 127
timing of exposures in ultrasonic hemorrhage of murine lung (Raeman), 507

ultrasound-induced enhancement of ACh, AChE and GABA in fetal brain tissue of mouse (Suneetha), 411

Indicator dilution
myocardial regional blood flow: quantitative measurement by computer analysis of contrast enhanced echocardiographic images (Mor-Avi), 619
myocardial transit time of the echocardiographic contrast media (Mor-Avi), 635

Inferior vena cava
flow velocity waveforms in the ductus venosus, umbilical vein and inferior vena cava in normal human fetuses at 12–15 weeks of gestation (Huisman), 441

Integrated backscatter
a feasibility study on quantitating myocardial perfusion with Albunex®, an ultrasonic contrast agent (Wilson), 181
non-Rayleigh first-order statistics of ultrasonic backscatter from normal myocardium (Clifford), 487
quantification of ultrasonic anisotropy in normal myocardium with lateral gain compensation of two-dimensional integrated backscatter images (Recchia), 497
ultrasonic tissue characterization of experimental venous intimal hyperplasia (Parsons), 299
ultrasound myocardial integrated backscatter signal processing: frequency domain versus time domain (Rijsterborgh), 211

Intimal hyperplasia
Doppler color flow images of iliofemoral graft end-to-side distal anastomotic models (Rittgers), 257
ultrasonic tissue characterization of experimental venous intimal hyperplasia (Parsons), 299

Intravascular ultrasound
timing of exposures in ultrasonic hemorrhage of murine lung (Raeman), 507

Intraventricular hemorrhage
adaptive multipurpose probe fixation device for use on newborns (Michel), 581

Irradiation
a comparison of hemolytic and sonochemical activity of ultrasonic cavitation in a rotating tube (Miller), 83
acoustic properties of lesions generated with an ultrasound therapy system (Bush), 789
applications of lipid-coated microbubble ultrasonic contrast to tumor therapy (Simon), 123
biological effects of high energy shock waves in mouse skeletal muscle: correlation between ^{31}P magnetic resonance spectroscopic and microscopic alterations (Smits), 399
biological effects of laser-induced shock waves: structural and functional cell damage *in vitro* (Doukas), 137
cell density dependence of the ultrasonic degassing of fixed erythrocyte suspensions (Brayman), 243

characterization of extracorporeal ablation of normal and tumor-bearing liver tissue by high intensity focused ultrasound (Sibille), 803
effects of pulsed ultrasound on the frog heart: I. Thresholds for changes in cardiac rhythm and aortic pressure (Dalecki), 385
effects of pulsed ultrasound on the frog heart: II. An investigation of heating as a potential mechanism (Dalecki), 391
focal spacing and near-field heating during pulsed high temperature ultrasound therapy (Damianou), 777
heating of guinea-pig fetal brain during exposure to pulsed ultrasound (Bosward), 415
histological changes in rat liver tumours treated with high-intensity focused ultrasound (Chen), 67
in vitro evaluation of gallstone dissolution with methyl-tert-butyl ether and ultrasound energy (McKinley), 375
lysis of erythrocytes by exposure to CW ultrasound (Carstensen), 147
morphological effects of pulsed ultrasound in the lung (Penney), 127
timing of exposures in ultrasonic hemorrhage of murine lung (Raeman), 507
temperature elevation in focused Gaussian ultrasonic beams at various insonation times (Filipczyński), 667
the effect of gas bubbles on the production of ultrasound hyperthermia at 0.75 MHz: a phantom study (Watmough), 231
the response of normal and malignant cells to ultrasound *in vitro* (Lejbkowicz), 75
ultrasonic gas body activation in *Elodea* leaves and the mechanical index (Miller), 343
ultrasound-induced enhancement of ACh, AChE and GABA in fetal brain tissue of mouse (Suneetha), 411

IVC
flow velocity waveforms in the ductus venosus, umbilical vein and inferior vena cava in normal human fetuses at 12–15 weeks of gestation (Huisman), 441

Iversen, H. K., see Nielsen, T. H.

J

James, D., see Clifford, L.

Jap, P. H. K., see Smits, G. A. H. J.

Jensen, J. A.: range/velocity limitations for time-domain blood velocity estimation, 741

Jets
quantification of regurgitant flow through bileaflet heart valve prostheses: theoretical and *in vitro* studies (Cape), 461

Johnston, K. W., see Bascom, P. A. J.

de Jong, N., ten Cate, F. J., Vletter, W. B. and Roelandt, J. R. T. C.: quantification of transpulmonary echocontrast effects, 279

de Jonge, A. B., see Journée, H. L.

Jorch, G., see Michel, E.

Joseph, A. E. A., see Ramnarine, K. V.

Journée, H. L. and de Jonge, A. B.: ultrasound myography: application in nerve conduction velocity assessment and muscle cooling, 561

Justin, J., see Kimitsuki, H.

Justin, J., see Parsons, R. E.

K

Kadado, T. R., see Downing, G. J.

Kakegawa, T., see Kimitsuki, H.

Kalisz, A., see Parsons, R. E.

Keller, B. B., see Dalecki, D.

Kelly, P., see Carstensen, E. L.

Keselbrener, L., see Mor-Avi, V.

Khizhnyak, E., see Watmough, D. J.

Kidney
intrarenal Doppler findings of upstream renal artery stenosis: a preliminary report (Özbek), 3

Kimitsuki, H., Parsons, R. E., Sigel, B., Feleppa, E. J., Golub, R. M., Justin, J., Machi, J., Rorke, M., Sokil-Melgar, J., Kodama, I., Kurohiji, T., Kakegawa, T. and Zaren, H. A.: effect of perfusion and blood content on ultrasonic backscattering of liver tissue, 39

Kitamura, H., see Parsons, R. E.

Kodama, I., see Kimitsuki, H.

Kossoff, G., see Bosward, K. L.

Kossoff, G., Griffiths, K. A., Garrett, W. J., Warren, P. S., Roberts, A. B. and Mitchell, J. M.: thickness of tissues intervening between the transducer and fetus and models for fetal exposure calculations in transvaginal sonography, 59

Kujawska, T., see Filipczyński, L.

Kumar, R. P. S., see Suneetha, N.

Kurohiji, T., see Kimitsuki, H.

L

Lakshmi, R., see Watmough, D. J.

Lancée, C. T., see Rijsterborgh, H.

Lange, S. C., see Simon, R. H.

Lasers
biological effects of laser-induced shock waves: structural and functional cell damage *in vitro* (Doukas), 137

Left ventricle
methodology for three-dimensional reconstruction of the left ventricle from transesophageal echocardiograms (Martin), 27

Lehmann, E. D., Hopkins, K. D. and Gosling, R. G.: aortic compliance measurements using Doppler ultrasound: *in vivo* biochemical correlates, 683

Lejbkowicz, F., Zwiran, M. and Salzberg, S.: the response of normal and malignant cells to ultrasound *in vivo*, 75

Levene, H., see Wilson, B.

Li, S., Hoskins, P. R., Anderson, T. and McDicken, W. N.: measurement of real velocity during pulsatile flow using time-averaged maximum frequency of Doppler ultrasound waveforms, 105

Li, S., McDicken, W. N. and Hoskins, P. R.: nonlinear propagation in Doppler ultrasound, 359

Li, S., McDicken, W. N. and Hoskins, P. R.: refraction in Doppler ultrasound, 593L

Lipids
aortic compliance measurements using Doppler ultrasound: *in vivo* biochemical correlates (Lehmann), 683

Lithotripsy
biological effects of high energy shock waves in mouse skeletal muscle: correlation between ^{31}P magnetic resonance spectroscopic and microscopic alterations (Smits), 399
morphological effects of pulsed ultrasound in the lung (Penney), 127
transient acoustic cavitation in gallstone fragmentation: a study of gallstones fragmented *in vivo* (Vakil), 331

Liver
acoustic properties of lesions generated with an ultrasound therapy system (Bush), 789
characterization of extracorporeal ablation of normal and tumor-bearing liver tissue by high intensity focused ultrasound (Sibille), 803

Lizzi, F. L., see Parsons, R. E.

Long, C. D., see Parsons, R. E.

Lu, D. S. K., see McKinley, C. A.

Lung
morphological effects of pulsed ultrasound in the lung (Penney), 127
quantification of transpulmonary echocontrast effects (de Jong), 279
timing of exposures in ultrasonic hemorrhage of murine lung (Raeman), 507

M

Machi, J., see Kimitsuki, H.

Magnetic resonance spectroscopy
biological effects of high energy shock waves in mouse skeletal muscle: correlation between ^{31}P magnetic resonance spectroscopic and microscopic alterations (Smits), 399

Magnin, I., see Finet, G.

Malignant cells
the response of normal and malignant cells to ultrasound *in vitro* (Lejbkowicz), 75

Maltby, K., see Penney, D. P.

Martin, P. J., Evans, D. H., Naylor, A. R. and Bell, P. R. F.: transcranial colour coded sonography as an aid to measurement of blood flow velocity in the basal cerebral arteries, 711

Martin, R. W., Bashein, G., Nessly, M. L. and Sheehan, F. H.: methodology for three-dimensional reconstruction of the left ventricle from transesophageal echocardiograms, 27

Mastik, F., see Rijsterborgh, H.

Maulik, D., see Downing, G. J.

Maurincomme, E., see Finet, G.

McAuliffe, D. J., see Doukas, A. G.

McDermott, B. A., see Bohs, L. N.

McDicken, W. N., see Li, S.

McKinley, C. A., Hunt, J. W., Ricketts, J., Lu, D. S. K., Ho, C.-S. and Foster, F. S.: *in vitro* evaluation of gallstone dissolution with methyl-tert-butyl ether and ultrasound energy, 375

Mean velocity
comparison of the performance of the RF cross correlation and Doppler autocorrelation technique to estimate the mean velocity of simulated ultrasound signals (Hoeks), 727
measurement of mean velocity during pulsatile flow using time-averaged maximum frequency of Doppler ultrasound waveforms (Li), 105
range/velocity limitations for time-domain blood velocity estimation (Jensen), 741

Mechanical index
ultrasonic gas body activation in *Elodea* leaves and the mechanical index (Miller), 343

Methyl-tert-butyl ether
in vitro evaluation of gallstone dissolution with methyl-tert-butyl ether and ultrasound energy (McKinley), 375

Mice
biological effects of high energy shock waves in mouse skeletal muscle: correlation between ^{31}P magnetic resonance spectroscopic and microscopic alterations (Smits), 399
morphological effects of pulsed ultrasound in the lung (Penney), 127
quantification of ventricular remodeling in the tight-skin mouse cardiomyopathy with acoustic microscopy (Wong), 365
timing of exposures in ultrasonic hemorrhage of murine lung (Raeman), 507
ultrasound-induced enhancement of ACh, AChE and GABA in fetal brain tissue of mouse (Suneetha), 411

Michel, E., Zernikow, B., Rabe, H. and Jorch, G.: adaptive multipurpose probe fixation device for use on newborns, 581

Mickelson, J. K., see Hartley, C. J.

Miller, D. L. and Thomas, R. M.: a comparison of hemolytic and sonochemical activity of ultrasonic cavitation in a rotating tube, 83

Miller, D. L. and Thomas, R. M.: ultrasonic gas body activation in *Elodea* leaves and the mechanical index, 343

Miller, J. G., see Recchia, D.

Miller, J. G., see Wong, A. K.

Miller, M. W., see Brayman, A. A.

Mitchell, J. M., see Kossoff, G.

Mitchell, R., see Picot, P. A.

Model

Doppler color flow images of iliofemoral graft end-to-side distal anastomotic models (Rittgers), 257

Doppler quantification of echo-contrast injections *in vivo* (Hartley), 269

estimation of *in situ* ultrasound exposure during obstetric examinations (Ramnarine), 319

in vitro evaluation of gallstone dissolution with methyl-tert-butyl ether and ultrasound energy (McKinley), 375

measurement of mean velocity during pulsatile flow using time-averaged maximum frequency of Doppler ultrasound waveforms (Li), 105

nonlinear propagation in Doppler ultrasound (Li), 359

on the Doppler signal from a steady flow asymmetrical stenosis model: effects of turbulence (Bascom), 197

quantification of regurgitant flow through bileaflet heart valve prostheses: theoretical and *in vitro* studies (Cape), 461

quantification of transpulmonary echocontrast effects (de Jong), 279

quantitative echo contrast concentration measurement by Doppler sonography (Schwarz), 289

the effect of gas bubbles on the production of ultrasound hyperthermia at 0.75 MHz: a phantom study (Watmough), 231

thickness of tissues intervening between the transducer and fetus and models for fetal exposure calculations in transvaginal sonography (Kossoff), 59

ultrasonic tissue characterization of experimental venous intimal hyperplasia (Parsons), 299

volumetric arterial flow quantification using echo contrast. An *in vitro* comparison of three ultrasonic intensity methods: radio frequency, video and Doppler (Schwarz), 447

Monitoring

adaptive multipurpose probe fixation device for use on newborns (Michel), 581

Mor-Avi, V., Akselrod, S., David, D., Keselbrener, L. and Bitton, Y.: myocardial transit time of the echocardiographic contrast media, 635

Mor-Avi, V., David, D., Akselrod, S., Bitton, Y. and Choshniak, I.: myocardial regional blood flow: quantitative measurement by computer analysis of contrast enhanced echocardiographic images, 619

Morrow, R. J., Bull, S. B. and Adamson, S. L.: experimentally induced changes in heart rate after umbilicoplacental hemodynamics in fetal sheep, 309

Mottley, J. G., see Schwarz, K. Q.

Mouse cells

biological effects of high energy shock waves in mouse skeletal muscle: correlation between ^{31}P magnetic resonance spectroscopic and microscopic alterations (Smits), 399

the response of normal and malignant cells to ultrasound *in vitro* (Lejbkowicz), 75

Movement detection
ultrasound myography: application in nerve conduction velocity assessment and muscle cooling (Journée), 561

MRI
the feasibility of using MRI to monitor and guide noninvasive surgery (Hynynen), 91L

Muscle cooling
ultrasound myography: application in nerve conduction velocity assessment and muscle cooling (Journée), 561

Myocardial perfusion
a feasibility study on quantitating myocardial perfusion with Albunex®, an ultrasonic contrast agent (Wilson), 181
Doppler quantification of echo-contrast injections *in vivo* (Hartley), 269
myocardial regional blood flow: quantitative measurement by computer analysis of contrast enhanced echocardiographic images (Mor-Avi), 619
myocardial transit time of the echocardiographic contrast media (Mor-Avi), 635

Myocardium
a feasibility study on quantitating myocardial perfusion with Albunex®, an ultrasonic contrast agent (Wilson), 181
Doppler quantification of echo-contrast injections *in vivo* (Hartley), 269
myocardial regional blood flow: quantitative measurement by computer analysis of contrast enhanced echocardiographic images (Mor-Avi), 619
myocardial transit time of the echocardiographic contrast media (Mor-Avi), 635
non-Rayleigh first-order statistics of ultrasonic backscatter from normal myocardium (Clifford), 487
ultrasound myocardial integrated backscatter signal processing: frequency domain versus time domain (Rijsterborgh), 211

Myocytes
biological effects of high energy shock waves in mouse skeletal muscle: correlation between ^{31}P magnetic resonance spectroscopic and microscopic alterations (Smits), 399

Myofiber
biological effects of high energy shock waves in mouse skeletal muscle: correlation between ^{31}P magnetic resonance spectroscopic and microscopic alterations (Smits), 399

Myography
ultrasound myography: application in nerve conduction velocity assessment and muscle cooling (Journée), 561

N

Nanda, N. C., see Cape, E. G.

Nanda, N. C., see Fan, P.

Nassiri, D. K., see Ramnarine, K. V.

Naylor, A. R., see Martin, P. J.

Neovascularity
temperature-dependent ultrasound color flow Doppler imaging in the study of a VX2 tumor in rabbits: preliminary findings (Shmulewitz), 221

Nerve conduction velocity
ultrasound myography: application in nerve conduction velocity assessment and muscle cooling (Journée), 561

Nessly, M. L., see Martin, R. W.

Neurotransmitters
ultrasound-induced enhancement of ACh, AChE and GABA in fetal brain tissue of mouse (Suneetha), 411

Newhouse, V. L., see Schrope, B. A.

Nielsen, T. H., Iversen, H. K., Tfelt-Hansen, P. and Olesen, J.: small arteries can be accurately studied *in vivo,* using high frequency ultrasound, 717

Non-Rayleigh statistics
non-Rayleigh first-order statistics of ultrasonic backscatter from normal myocardium (Clifford), 487

Nonaxial flow
a real time system for quantifying and displaying two-dimensional velocities using ultrasound (Bohs), 751

Nonlinear effects
acoustic streaming generated by a focused Gaussian beam and finite amplitude tonebursts (Wu), 167

Nonlinear propagation
effects of pulsed ultrasound on the frog heart: II. An investigation of heating as a potential mechanism (Dalecki), 391
nonlinear propagation in Doppler ultrasound (Li), 359

O

Olesen, J., see Nielsen, T. H.

Oosterhof, G. O. N., see Smits, G. A. H. J.

Oosterveld, B. J., see Thijssen, J. M.

Oosterveld, B. J., Thijssen, J. M., Hartman, P. C. and Rosenbusch, G. J. E.: detection of diffuse liver disease by quantitative echography: dependence on *a priori* choice of parameters, 21

Ophthalmology
the history of ultrasound techniques in ophthalmology (Thijssen), 599

Osborn, T. G., see Wong, A. K.

Ovary
endovaginal pulsed and color Doppler in first-trimester pregnancy (Dillon), 517

Özbek, S. S., Aytac, S. K., Erden, M. I. and Sanlidilek, N. U.: intrarenal Doppler findings of upstream renal artery stenosis: a preliminary report, 3

P

Parsons, R. E., Sigel, B., Feleppa, E. J., Golub, R. M., Justin, J., Swami, V. K., Rorke, M., Kalisz, A., Long, C. D., Can, A., Lizzi, F. L. and Kitamura, H.: ultrasonic tissue characterization of experimental venous intimal hyperplasia, 299

Parsons, R. E., see Kimitsuki, H.

Pashovkin, T. N., see Watmough, D. J.

Patel, R. H., see Ramnarine, K. V.

Pearce, J. M., see Ramnarine, K. V.

Penney, D. P., Schenk, E. A., Maltby, K., Hartman-Raeman, C., Child, S. Z. and Carstensen, E. L.: morphological effects of pulsed ultrasound in the lung, 127

Perfusion
a feasibility study on quantitating myocardial perfusion with Albunex®, an ultrasonic contrast agent (Wilson), 181
Doppler quantification of echo-contrast injections *in vivo* (Hartley), 269
methodology for three-dimensional reconstruction of the left ventricle from transesophageal echocardiograms (Martin), 27
quantification of transpulmonary echocontrast effects (de Jong), 279
quantitative echo contrast concentration measurement by Doppler sonography (Schwarz), 289
second harmonic ultrasonic blood perfusion measurement (Schrope), 567
temperature-dependent ultrasound color flow Doppler imaging in the study of a VX2 tumor in rabbits: preliminary findings (Shmulewitz), 221

Peripheral arteries
three-dimensional colour Doppler imaging (Picot), 95

Peripheral vascular resistance
in vivo correlation of Doppler waveform analysis with arterial input impedance parameters (Downing), 549

Phase aberration
correction of phase aberrations for sectored annular array ultrasound transducers (Gambetti), 763

Phillips, C., see Downing, G. J.

PI
in vivo correlation of Doppler waveform analysis with arterial input impedance parameters (Downing), 549
transcranial colour coded sonography as an aid to measurement of blood flow velocity in the basal cerebral arteries (Martin), 711

Picot, P. A., Rickey, D. W., Mitchell, R., Rankin, R. N. and Fenster, A.: three-dimensional colour Doppler imaging, 95

Piepgras, A., Bise, K. and Schmiedek, P.: morphometry of intraluminal side-to-side differences in human basal cerebral arteries, 193

Pignoli, P., see Tortoli, P.

Placental flow
experimentally induced changes in heart rate alter umbilicoplacental hemodynamics in fetal sheep (Morrow), 309

Podobnik, M., Singer, Z., Ciglar, S. and Bulic, M.: preoperative diagnosis of primary fallopian tube carcinoma by transvaginal ultrasound, cytological finding and CA-125, 587

Ponchon, T., see Sibille, A.

Power spectrum
effect of perfusion and blood content on ultrasonic backscattering of liver tissue (Kimitsuki), 39

Prat, F., see Sibille, A.

Pregnancy
endovaginal pulsed and color Doppler in first-trimester pregnancy (Dillon), 517
estimation of *in situ* ultrasound exposure during obstetric examinations (Ramnarine), 319

Primary fallopian tube carcinoma
preoperative diagnosis of primary fallopian tube carcinoma by transvaginal ultrasound, cytological finding and CA-125 (Podobnik), 587

Probe fixation
adaptive multipurpose probe fixation device for use on newborns (Michel), 581

Prostheses
quantification of regurgitant flow through bileaflet heart valve prostheses: theoretical and *in vitro* studies (Cape), 461

Pulmonary trunk
relationship between fetal pulmonary trunk and ductus arteriosus flow velocity waveforms in early normal pregnancy (Brezinka), 527

Pulsatile flow
Doppler color flow images of iliofemoral graft end-to-side distal anastomotic models (Rittgers), 257
measurement of mean velocity during pulsatile flow using time-averaged maximum frequency of Doppler ultrasound waveforms (Li), 105

Pulse wave velocity
aortic compliance measurements using Doppler ultrasound: *in vivo* biochemical correlates (Lehmann), 683

Q

Quan, K. M., see Watmough, D. J.

R

Rabe, H., see Michel, E.

Radiofrequency
volumetric arterial flow quantification using echo contrast. An *in vitro* comparison of three ultrasonic intensity methods: radio frequency, video and Doppler (Schwarz), 447

Raeman, C. H., Child, S. Z. and Carstensen, E. L.: timing of exposure in ultrasonic hemorrhage of murine lung, 507

Raeman, C. H., see Carstensen, E. L.

Raeman, C. H., see Dalecki, D.

Ramnarine, K. V., Nassiri, D. K., Pearce, J. M., Joseph, A. E. A., Patel, R. H. and Varma, T. R.: estimation of *in situ* ultrasound exposure during obstetric examinations, 319

Ramos, I. M., see Dillon, E. H.

Range/velocity limitation
range/velocity limitations for time-domain blood velocity estimation (Jensen), 741

Rankin, R. N., see Picot, P. A.

Rats
applications of lipid-coated microbubble ultrasonic contrast to tumor therapy (Simon), 123
histological changes in rat liver tumours treated with high-intensity focused ultrasound (Chen), 67

Recchia, D., Miller, J. G. and Wickline, S. A.: quantification of ultrasonic anisotropy in normal myocardium with lateral gain compensation of two-dimensional integrated backscatter images, 497

Refraction
refraction in Doppler ultrasound (Li), 593L

Regurgitation
quantification of regurgitant flow through bileaflet heart valve prostheses: theoretical and *in vitro* studies (Cape), 461

Renal artery
intrarenal Doppler findings of upstream renal artery stenosis: a preliminary report (Özbek), 3

Renal circulation
intrarenal Doppler findings of upstream renal artery stenosis: a preliminary report (Özbek), 3

Reneman, R. S., see Hoeks, A. P. G.

Retrospective diagnosis
detection of diffuse liver disease by quantitative echography: dependence on *a priori* choice of parameters (Oosterveld), 21

Reviews, book
Abdominal sonography: Sauerbrei, Nguyen and Nolan (Scharling), 425
Annual of genitourinary radiology and ultrasound: Pollack and Goldstein (Hissong), 425
Atlas of color-coded Doppler sonography: Fruhwald and Blackwell (Weill), 427
Doppler ultrasound in perinatal medicine: Pearce (Veille), 595
Intravascular ultrasound imaging: Cavaye and White (Strandness), 595
Introduction to vascular scanning: Ridgway (Burnham), 513

Techniques of venous imaging/Venous imaging technique: Talbot and Oliver (Daniel), 513
The search for Christian Doppler: Eden (Kremkau), 426
Output measurements for medical ultrasound: Preston (Harris), 426

RF B-mode
correlations between acoustic and texture parameters from RF and B-mode liver echograms (Thijssen), 13

Ricketts, J., see McKinley, C. A.

Rickey, D. W., see Picot, P. A.

Riddler, S., see Chen, L.

Rijsterborgh, H., Mastik, F., Lancée, C. T., Verdouw, P., Roelandt, J. and Bom, N.: ultrasound myocardial integrated backscatter signal processing: frequency domain versus time domain, 211

Rittgers, S. E. and Bhambhani, G. H.: Doppler color flow images of iliofemoral graft end-to-side distal anastomotic models, 257

Rivens, I., see Bush, N. L.

Rivens, I., see Chen, L.

Roberts, A. B., see Kossoff, G.

Roelandt, J. R. T. C., see de Jong, N.

Roelandt, J., see Rijsterborgh, H.

Roriz, R., see Finet, G.

Rorke, M., see Kimitsuki, H.

Rorke, M., see Parsons, R. E.

Rosenbusch, G. J. E., see Oosterveld, B. J.

Rosenbusch, G. J. E., see Thijssen, J. M.

Rosenthal, S. M., see Fan, P.

Routh, H. F., see Bascom, P. A. J.

S

Safety
acoustic streaming generated by a focused Gaussian beam and finite amplitude tonebursts (Wu), 167
estimation of *in situ* ultrasound exposure during obstetric examinations (Ramnarine), 319
heating of guinea-pig fetal brain during exposure to pulsed ultrasound (Bosward), 415
temperature elevation in focused Gaussian ultrasonic beams at various insonation times (Filipczyński), 667
the effect of gas bubbles on the production of ultrasound hyperthermia at 0.75 MHz: a phantom study (Watmough), 231
the history of ultrasound techniques in ophthalmology (Thijssen), 599
ultrasonic gas body activation in *Elodea* leaves and the mechanical index (Miller), 343

Salzberg, S., see Lejbkowicz, F.

Sanlidilek, N. U., see Özbek, S. S.

Sarvazyan, A. P., see Watmough, D. J.

Scanner characteristics
compensation for the signal processing characteristics of ultrasound B-mode scanners in adaptive speckle reduction (Crawford), 469

Scattering
a feasibility study on quantitating myocardial perfusion with Albunex®, an ultrasonic contrast agent (Wilson), 181
acoustic properties of lesions generated with an ultrasound therapy system (Bush), 789
detection of diffuse liver disease by quantitative echography: dependence on *a priori* choice of parameters (Oosterveld), 21
Doppler quantification of echo-contrast injections *in vivo* (Hartley), 269
effect of perfusion and blood content on ultrasonic backscattering of liver tissue (Kimitsuki), 39
on the Doppler signal from a steady flow asymmetrical stenosis model: effects of turbulence (Bascom), 197
quantification of transpulmonary echocontrast effects (de Jong), 279
quantification of ultrasonic anisotropy in normal myocardium with lateral gain compensation of two-dimensional integrated backscatter images (Recchia), 497
quantification of ventricular remodeling in the tight-skin mouse cardiomyopathy with acoustic microscopy (Wong), 365
quantitative echo contrast concentration measurement by Doppler sonography (Schwarz), 289
ultrasonic tissue characterization of experimental venous intimal hyperplasia (Parsons), 299
ultrasound myocardial integrated backscatter signal processing: frequency domain versus time domain (Rijsterborgh), 211

Schalken, J. A., see Smits, G. A. H. J.

Schenck, J. F., see Hynynen, K.

Schenk, E. A., see Penney, D. P.

Schery, L., see Carstensen, E. L.

Schlief, R., see Schwarz, K. Q.

Schmiedek, P., see Piepgras, A.

Schrope, B. A. and Newhouse, V. L.: second harmonic ultrasonic blood perfusion measurement, 567

Schwarz, K. Q., Bezante, G. P., Chen, X., Mottley, J. G. and Schlief, R.: volumetric arterial flow quantification using echo contrast. An *in vitro* comparison of three ultrasonic intensity methods: radio frequency, video and Doppler, 447

Schwarz, K. Q., Bezante, G. P., Chen, X. and Schlief, R.: quantitative echo contrast concentration measurement by Doppler sonography, 289

Second harmonic
second harmonic ultrasonic blood perfusion measurement (Schrope), 567

Sectored annular arrays
correction of phase aberrations for sectored annular array ultrasound transducers (Gambetti), 763

Sheehan, F. H., see Martin, R. W.

Shmulewitz, A., Teefey, S. A., Coldwell, D. and Starr, F. L., III.: temperature-dependent ultrasound color flow Doppler imaging in the study of a VX2 tumor in rabbits: preliminary findings, 221

Shock waves
biological effects of laser-induced shock waves: structural and functional cell damage *in vitro* (Doukas), 137

Shung, K. K., see Wilson, B.

Sibille, A., Prat, F., Chapelon, J.-Y., El Fadil, F. A., Henry, L., Theilliere, Y., Ponchon, T. and Cathignol, D.: characterization of extracorporeal ablation of normal and tumor-bearing liver tissue by high intensity focused ultrasound, 803

Sigel, B., see Parsons, R. E.

Sigel, B., see Kimitsuki, H.

Signal processing
a feasibility study on quantitating myocardial perfusion with Albunex®, an ultrasonic contrast agent (Wilson), 181
ultrasonic tissue characterization of experimental venous intimal hyperplasia (Parsons), 299
ultrasound myocardial integrated backscatter signal processing: frequency domain versus time domain (Rijsterborgh), 211

Simon, R. H., Ho, S.-Y., Lange, S. C., Uphoff, D. F. and D'Arrigo, J. S.: applications of lipid-coated microbubble ultrasonic contrast to tumor therapy, 123

Singer, Z., see Podobnik, M.

Smits, G. A. H. J., Jap, P. H. K., Heerschap, A., Oosterhof, G. O. N., Debruyne, F. M. J. and Schalken, J. A.: biological effects of high energy shock waves in mouse skeletal muscle: correlation between ^{31}P magnetic resonance spectroscopic and microscopic alterations, 399

Sokil-Melgar, J., see Kimitsuki, H.

Sound speed
acoustic properties of lesions generated with an ultrasound therapy system (Bush), 789
correction of phase aberrations for sectored annular array ultrasound transducers (Gambetti), 763

Speckle
compensation for the signal processing characteristics of ultrasound B-mode scanners in adaptive speckle reduction (Crawford), 469
correction of phase aberrations for sectored annular array ultrasound transducers (Gambetti), 763
Doppler ultrasound spectral shape in the poststenotic velocity field (Hutchison), 649
nonlinear propagation in Doppler ultrasound (Li), 359
transverse Doppler spectral analysis for a correct interpretation of flow sonograms (Tortoli), 115
ultrasonic tissue characterization of experimental venous intimal hyperplasia (Parsons), 299

Spectral broadening
Doppler ultrasound spectral shape in the poststenotic velocity field (Hutchison), 649

Starr, F. L., III, see Shmulewitz, A.

Stenosis
Doppler ultrasound spectral shape in the poststenotic velocity field (Hutchison), 649
intrarenal Doppler findings of upstream renal artery stenosis: a preliminary report (Özbek), 3
on the Doppler signal from a steady flow asymmetrical stenosis model: effects of turbulence (Bascom), 197

Stewart, P. A., see Huisman, T. W. A.

Stewart, P. A., see Wladimiroff, J. W.

Stijnen, T., see Brezinka, C.

Stijnen, T., see Huisman, T. W. A.

Streaming
acoustic streaming generated by a focused Gaussian beam and finite amplitude tonebursts (Wu), 167

Suneetha, N. and Kumar, R. P. S.: ultrasound-induced enhancement of ACh, AChE and GABA in fetal brain tissue of mouse, 411

Surgery
acoustic properties of lesions generated with an ultrasound therapy system (Bush), 789
characterization of extracorporeal ablation of normal and tumor-bearing liver tissue by high intensity focused ultrasound (Sibille), 803
focal spacing and near-field heating during pulsed high temperature ultrasound therapy (Damianou), 777
the feasibility of using MRI to monitor and guide noninvasive surgery (Hynynen), 91L
the response of normal and malignant cells to ultrasound *in vitro* (Lejbkowicz), 75

Swami, V. K., see Parsons, R. E.

T

Tabib, A., see Finet, G.

Taylor, K. J. W., see Dillon, E. H.

Teefey, S. A., see Shmulewitz, A.

Temperature elevation
focal spacing and near-field heating during pulsed high temperature ultrasound therapy (Damianou), 777
heating of guinea-pig fetal brain during exposure to pulsed ultrasound (Bosward), 415
temperature elevation in focused Gaussian ultrasonic beams at various insonation times (Filipczyński), 667
the effect of gas bubbles on the production of ultrasound hyperthermia at 0.75 MHz: a phantom study (Watmough), 231

Ten Cate, F. J., see de Jong, N.

Texture analysis
correlations between acoustic and texture parameters from RF and B-mode liver echograms (Thijssen), 13
detection of diffuse liver disease by quantitative echography: dependence on *a priori* choice of parameters (Oosterveld), 21

Tfelt-Hansen, P., see Nielsen, T. H.

Theilliere, Y., see Sibille, A.

Therapeutic ultrasound
acoustic properties of lesions generated with an ultrasound therapy system (Bush), 789
applications of lipid-coated microbubble ultrasonic contrast to tumor therapy (Simon), 123
characterization of extracorporeal ablation of normal and tumor-bearing liver tissue by high intensity focused ultrasound (Sibille), 803
focal spacing and near-field heating during pulsed high temperature ultrasound therapy (Damianou), 777
histological changes in rat liver tumours treated with high-intensity focused ultrasound (Chen), 67
in vitro evaluation of gallstone dissolution with methyl-tert-butyl ether and ultrasound energy (McKinley), 375
the history of ultrasound techniques in ophthalmology (Thijssen), 599

Thermal effects
characterization of extracorporeal ablation of normal and tumor-bearing liver tissue by high intensity focused ultrasound (Sibille), 803
effects of pulsed ultrasound on the frog heart: I. Thresholds for changes in cardiac rhythm and aortic pressure (Dalecki), 385
effects of pulsed ultrasound on the frog heart: II. An investigation of heating as a potential mechanism (Dalecki), 391
focal spacing and near-field heating during pulsed high temperature ultrasound therapy (Damianou), 777
heating of guinea-pig fetal brain during exposure to pulsed ultrasound (Bosward), 415
the effect of gas bubbles on the production of ultrasound hyperthermia at 0.75 MHz: a phantom study (Watmough), 231

Thijssen, J. M., Oosterveld, B. J., Hartman, P. C. and Rosenbusch, G. J. E.: correlations between acoustic and texture parameters from RF and B-mode liver echograms, 13

Thijssen, J. M.: the history of ultrasound techniques in ophthalmology, 599

Thijssen, J. M., see Oosterveld, B. J.

Thomas, R. M., see Miller, D. L.

Three-dimensional imaging
methodology for three-dimensional reconstruction of the left ventricle from transesophageal echocardiograms (Martin), 27
three-dimensional colour Doppler imaging (Picot), 95

Thymidine incorporation
biological effects of laser-induced shock waves: structural and functional cell damage *in vitro* (Doukas), 137

Time domain
ultrasound myocardial integrated backscatter signal processing: frequency domain versus time domain (Rijsterborgh), 211

Tissue characterisation
acoustic properties of lesions generated with an ultrasound therapy system (Bush), 789
effect of perfusion and blood content on ultrasonic backscattering of liver tissue (Kimitsuki), 39
endovaginal pulsed and color Doppler in first-trimester pregnancy (Dillon), 517
non-Rayleigh first-order statistics of ultrasonic backscatter from normal myocardium (Clifford), 487
quantification of ventricular remodeling in the tight-skin mouse cardiomyopathy with acoustic microscopy (Wong), 365
quantification of ultrasonic anisotropy in normal myocardium with lateral gain compensation of two-dimensional integrated backscatter images (Recchia), 497
temperature-dependent ultrasound color flow Doppler imaging in the study of a VX2 tumor in rabbits: preliminary findings (Shmulewitz), 221
the history of ultrasound techniques in ophthalmology (Thijssen), 599
ultrasonic tissue characterization of experimental venous intimal hyperplasia (Parsons), 299

Tortoli, P., Guidi, G. and Pignoli, P.: transverse Doppler spectral analysis for a correct interpretation of flow sonograms, 115

Trahey, G. E., see Bohs, L. N.

Transcranial Doppler sonography
morphometry of intraluminal side-to-side differences in human basal cerebral arteries (Piepgras), 193
transcranial colour coded sonography as an aid to measurement of blood flow velocity in the basal cerebral arteries (Martin), 711

Transit time
myocardial regional blood flow: quantitative measurement by computer analysis of contrast enhanced echocardiographic images (Mor-Avi), 619
myocardial transit time of the echocardiographic contrast media (Mor-Avi), 635

Transoesophageal imaging
flow velocity waveforms in the ductus venosus, umbilical vein and inferior vena cava in normal human fetuses at 12–15 weeks of gestation (Huisman), 441
methodology for three-dimensional reconstruction of the left ventricle from transesophageal echocardiograms (Martin), 27

Transvaginal
endovaginal pulsed and color Doppler in first-trimester pregnancy (Dillon), 517
flow velocity waveforms in the ductus venosus, umbilical vein and inferior vena cava in normal human fetuses at 12–15 weeks of gestation (Huisman), 441
preoperative diagnosis of primary fallopian tube carcinoma by transvaginal ultrasound, cytological finding and CA-125 (Podobnik), 587

thickness of tissues intervening between the transducer and fetus and models for fetal exposure calculations in transvaginal sonography (Kossoff), 59

Transverse Doppler
transverse Doppler spectral analysis for a correct interpretation of flow sonograms (Tortoli), 115

Tumour imaging
temperature-dependent ultrasound color flow Doppler imaging in the study of a VX2 tumor in rabbits: preliminary findings (Shmulewitz), 221

Tumour surgery
acoustic properties of lesions generated with an ultrasound therapy system (Bush), 789
applications of lipid-coated microbubble ultrasonic contrast to tumor therapy (Simon), 123
characterization of extracorporeal ablation of normal and tumor-bearing liver tissue by high intensity focused ultrasound (Sibille), 803
histological changes in rat liver tumours treated with high-intensity focused ultrasound (Chen), 67

Tumours
applications of lipid-coated microbubble ultrasonic contrast to tumor therapy (Simon), 123
histological changes in rat liver tumours treated with high-intensity focused ultrasound (Chen), 67
temperature-dependent ultrasound color flow Doppler imaging in the study of a VX2 tumor in rabbits: preliminary findings (Shmulewitz), 221

Turbulence
Doppler ultrasound spectral shape in the poststenotic velocity field (Hutchison), 649
on the Doppler signal from a steady flow asymmetrical stenosis model: effects of turbulence (Bascom), 197
quantification of regurgitant flow through bileaflet heart valve prostheses: theoretical and *in vitro* studies (Cape), 461

Two-dimensional array
correction of phase aberrations for sectored annular array ultrasound transducers (Gambetti), 763

U

Umbilical flow
experimentally induced changes in heart rate alter umbilicoplacental hemodynamics in fetal sheep (Morrow), 309
flow velocity waveforms in the ductus venosus, umbilical vein and inferior vena cava in normal human fetuses at 12–15 weeks of gestation (Huisman), 441

Unger, E., see Hynynen, K.

Uphoff, D. F., see Simon, R. H.

Uterine artery
endovaginal pulsed and color Doppler in first-trimester pregnancy (Dillon), 517

V

Vakil, N. and Everbach, E. C.: transient acoustic cavitation in gallstone fragmentation: a study of gallstones fragmented *in vivo*, 331

Varma, T. R., see Ramnarine, K. V.

Vascular input impedance
in vivo correlation of Doppler waveform analysis with arterial input impedance parameters (Downing), 549

Vascularity
histological changes in rat liver tumours treated with high-intensity focused ultrasound (Chen), 67
temperature-dependent ultrasound color flow Doppler imaging in the study of a VX2 tumor in rabbits: preliminary findings (Shmulewitz), 221

Vector velocity
a real time system for quantifying and displaying two-dimensional velocities using ultrasound (Bohs), 751

Velocity flow indices
experimentally induced changes in heart rate alter umbilicoplacental hemodynamics in fetal sheep (Morrow), 309
on the Doppler signal from a steady flow asymmetrical stenosis model: effects of turbulence (Bascom), 197

Velocity waveforms
endovaginal pulsed and color Doppler in first-trimester pregnancy (Dillon), 517
flow velocity waveforms in the ductus venosus, umbilical vein and inferior vena cava in normal human fetuses at 12–15 weeks of gestation (Huisman), 441
in vivo correlation of Doppler waveform analysis with arterial input impedance parameters (Downing), 549
measurement of mean velocity during pulsatile flow using time-averaged maximum frequency of Doppler ultrasound waveforms (Li), 105

Venous thrombosis
ultrasonic tissue characterization of experimental venous intimal hyperplasia (Parsons), 299

Ventricular performance
methodology for three-dimensional reconstruction of the left ventricle from transesophageal echocardiograms (Martin), 27
quantification of ventricular remodeling in the tight-skin mouse cardiomyopathy with acoustic microscopy (Wong), 365

Verdouw, P., see Rijsterborgh, H.

Video intensity
volumetric arterial flow quantification using echo contrast. An *in vitro* comparison of three ultrasonic intensity methods: radio frequency, video and Doppler (Schwarz), 447

Vletter, W. B., see de Jong, N.

W

Wang, W.-Q., see Wang, Y.-Y.

Wang, Y.-Y. and Wang, W.-Q.: fractal concept and its analysis method for Doppler ultrasound signals, 661

Warren, P. S., see Kossoff, G.

Watmough, J. A., see Watmough, D. J.

Watmough, D. J., Lakshmi, R., Ghezzi, F., Quan, K. M., Watmough, J. A., Khizhnyak, E., Pashovkin, T. N. and Sarvazyan, A. P.: the effect of gas bubbles on the production of ultrasound hyperthermia at 0.75 MHz: a phantom study, 231

Wickline, S. A., see Recchia, D.

Wickline, S. A., see Wong, A. K.

Wilson, B., Shung, K. K., Hete, B., Levene, H. and Barnhart, J. L.: a feasibility study on quantitating myocardial perfusion with Albunex®, an ultrasonic contrast agent, 181

Wladimiroff, J. W., Heydanus, R. and Stewart, P. A.: Doppler colour flow mapping of fetal intracerebral arteries in the presence of central nervous system anomalies, 355

Wladimiroff, J. W., see Brezinka, Ch.

Wladimiroff, J. W., see Huisman, T. W. A.

Wojcik, J., see Filipczyński, L.

Wong, A. K., Osborn, T. G., Miller, J. G. and Wickline, S. A.: quantification of ventricular remodeling in the tight-skin mouse cardiomyopathy with acoustic microscopy, 365

Wood, A. K. W., see Bosward, K. L.

Wu, J. and Du, G.: acoustic streaming generated by a focused Gaussian beam and finite amplitude tonebursts, 167

Y

Yoganathan, A. P., see Cape, E. G.

Yoganathan, A., see Fan, P.

Z

Zaren, H. A., see Kimitsuki, H.

Zernikow, B., see Michel, E.

Zwiran, M., see Lejbkowicz, F.

MAGNETIC RESONANCE IMAGING

Editor:
JOHN C. GORE,
Department of Diagnostic Imaging, Yale University School of Medicine, 333 Cedar Street, New Haven, CT 06510, USA

An International Journal of Basic Research and Clinical Applications

Magnetic Resonance Imaging provides outstanding, peer-reviewed articles reporting on:

- Clinical MRI
- Functional Imaging
- MR Angiography and the latest Technical Developments
- Contrast Agents
- NMR Physics and Relaxation
- NMR Microscopy
- *In Vivo* Spectroscopy
- Reviews

As of 1993, MRI has incorporated *Reviews of Magnetic Resonance in Medicine* into its regular format. Past Reviews include *Artifacts in Magnetic Resonance Imaging*, by R. Henkleman & M.J. Bronskill, and *A Comprehensive Technical Review of Short TR Fast MRI*, by E.M. Haacke, P.A. Wielopolski & J.T. Koch. Most recently, MRI published *Gradient Coil Design: A Review of Methods*, by R. Turner.

Previously published six issues per year, MRI has increased its frequency to eight times per year to maintain rapid publication times and to better serve its readership.

FREE SAMPLE COPY AVAILABLE UPON REQUEST

PERGAMON
An imprint of Elsevier Science

US: 660 White Plains Road
Tarrytown, NY 10591-5153

UK: The Boulevard, Langford Lane,
Kidlington, Oxford OX5 1GB

RECENT ARTICLES

F. Ståhlberg (Sweden), L. Søndergaard, C. Thomsen & O. Henriksen (Denmark), Quantification of complex flow using MR phase imaging—A study of parameters influencing the phase/velocity relation.

P. Wedeking, C.H. Sotak, J. Telser, K. Kumar, C.A. Chang & M.F. Tweedle (USA), Quantitative dependence of MR signal intensity on tissue concentration of Gd(HP-DO34) in the nephrectomized rat.

J.W. Hugg, G.B. Matson, D.B. Tweig, A.A. Maudsley (USA), D. Sappey-Marinier (France) & M.W. Weiner (USA), Phosphorus-31 MR spectroscopic imaging (MRSI) of normal and pathological human brains.

R. Pascone, T. Vullo, J. Farrell & P.T. Cahill (USA), Explicit treatment of mutual inductance in eight-column birdcage resonators.

R.T. Constable, A.W. Anderson, J. Zhong & J.C. Gore (USA), Factors influencing contrast in fast spin-echo MR imaging.

INDEXED/ABSTRACTED IN

Current Contents/Clinical Medicine, CABS, BIOSIS Database, Excerpta Medica, Electron & Commun Abstr, Chemical Abstr, INSPEC Database, Index Medicus, MEDLINE, MEDLARS, Index of European Radiological Journals, Reference Update

SUBSCRIPTION INFORMATION

687/ISSN: 0730-725X Volume 12, 1994
8 Issues Per Annum

Personal Rate (1994) *£ 48.00/US$ 74.00

Annual Institutional Rate (1994) *£362.00/US$555.00

*Sterling prices quoted apply worldwide, except in the Americas. US dollar prices quoted apply in the Americas only. Prices include postage and insurance.

Subscribe to a journal that offers computer applications in the biosciences and in medicine . . .

COMPUTERS IN BIOLOGY AND MEDICINE

An International Journal

EDITOR-IN-CHIEF

ROBERT S. LEDLEY, National Biomedical Research Foundation, Georgetown University Medical Center, 3900 Reservoir Road, NW Washington, DC 20007 USA

AIMS AND SCOPE

This journal is a medium of international communication on the revolutionary advances being made in the application of the computer to the fields of biomedical engineering and medical informatics. It encourages the exchange of research, instruction, ideas and information on all aspects of the growing use of computers and focuses on such areas as:

(1) Analysis of biomedical systems: solutions of equations
(2) Synthesis of biomedical systems: simulations
(3) Special medical data processing methods
(4) Special purpose computers and clinical data processing
(5) Medical diagnosis and record processing.

RECENT ARTICLES

A.W. ELBERN (Brazil), Computation of dose distribution for linear radioactive sources in brachytherapy.
S. ABBOUD, A. ALALUF, S. EINAV & D. SADEH (Israel), Real-time abdominal fetal ECG recording using a hardware correlator.
B. DAVISON, J. GUMOWITZ & E. INGENITO (USA), Development and testing of a PC-based system with menu-driven software for evaluating lung function in ICU patients.
N. PRADHAN, D. NARAYANA DUTT & S. SATYAM (India), A mimetic-based frequency domain technique for automatic generation of EEG reports.
T.D. LAGERLUND & P.A. LOW (USA), Mathematical modeling of time-dependent oxygen transport in rat peripheral nerve.
C. BLINCOE (USA), Computer simulation of normal and pathological copper metabolism in man.
L.B. SCHWARTZ, C.M. PURUT, D.M. CRAIG, P.K. SMITH & R.L. McCANN (USA), Computer-assisted modeling of blood-flow: Theoretical evidence for the existence of optimal flow wave patterns.
R.D. MILLER & T.J. WITEK, JR. (USA), An algorithm for measurement of expiratory flow rate parameters on the partial expiratory flow-volume curve.
T.W. BLACKSTAD, T. KARAGÜLLE, M.S. MALMIERCA & K.K. OSEN (Norway), Computer methods in neuroanatomy: Determining mutual orientation of whole neuronal arbors.

INDEXED IN

Current Contents/Life Sciences, Current Contents/Health Services Administration, Current Contents/Engineering, Technology & Applied Sciences, Index Medicus, MEDLINE, MEDLARS, CABS, BIOSIS Database, Engrg Ind Monthly and Author Index, Computer Contents, PASCAL/CNRS Database, INSPEC

SUBSCRIPTION INFORMATION

Volume 24, 1994 351/ISSN: 0010-4825 Published 6 issues per annum
Annual Subscription Rate (1994) *£364.00/US$560.00
Associated Personal Rate (1994) *£100.00/US$156.00

*Sterling prices quoted apply worldwide, except in the Americas. US dollar prices apply in the Americas only. Prices include postage and insurance.

Free sample copy available upon request.

PERGAMON
An Imprint of Elsevier Science

US: 660 White Plains Road, Tarrytown, NY 10591-5153
UK: The Boulevard, Langford Lane, Kidlington, Oxford OX5 1GB